

Dissolution of Fluoride Salts in Hanford Tank Waste

July 2020

LA Mahoney
MS Fountain
CA Burns

DISCLAIMER

This report was prepared as an account of work sponsored by an agency of the United States Government. Neither the United States Government nor any agency thereof, nor Battelle Memorial Institute, nor any of their employees, makes **any warranty, express or implied, or assumes any legal liability or responsibility for the accuracy, completeness, or usefulness of any information, apparatus, product, or process disclosed, or represents that its use would not infringe privately owned rights.** Reference herein to any specific commercial product, process, or service by trade name, trademark, manufacturer, or otherwise does not necessarily constitute or imply its endorsement, recommendation, or favoring by the United States Government or any agency thereof, or Battelle Memorial Institute. The views and opinions of authors expressed herein do not necessarily state or reflect those of the United States Government or any agency thereof.

PACIFIC NORTHWEST NATIONAL LABORATORY
operated by
BATTELLE
for the
UNITED STATES DEPARTMENT OF ENERGY
under Contract DE-AC05-76RL01830

Printed in the United States of America

Available to DOE and DOE contractors from the
Office of Scientific and Technical Information,
P.O. Box 62, Oak Ridge, TN 37831-0062;
ph: (865) 576-8401
fax: (865) 576-5728
email: reports@adonis.osti.gov

Available to the public from the National Technical Information Service
5301 Shawnee Rd., Alexandria, VA 22312
ph: (800) 553-NTIS (6847)
email: orders@ntis.gov <<https://www.ntis.gov/about>>
Online ordering: <http://www.ntis.gov>

Dissolution of Fluoride Salts in Hanford Tank Waste

July 2020

LA Mahoney
MS Fountain
CA Burns

Prepared for
the U.S. Department of Energy
under Contract DE-AC05-76RL01830

Pacific Northwest National Laboratory
Richland, Washington 99354

Summary

The Direct Feed High-Level Waste (DFHLW) strategy represents one alternative flowsheet seeking to bypass the Hanford Waste Treatment and Immobilization Plant Pretreatment Facility while retaining some key processing functions oriented towards maximization of waste feed loading and minimization of high-level waste (HLW) volume. The DFHLW flowsheet thus needs some level of leaching, washing, and solids concentration, which could occur in a new facility or potentially in double-shell tanks (DSTs). The effectiveness and efficiency of sludge washing has a substantial impact on DST space, mission duration, and the required evaporation and low-activity waste (LAW) treatment operations associated with these large wash-water additions.

One target species requiring washing is fluoride. Fluoride, commonly present in many high-level wastes at Hanford, is found predominantly in the form of fluoride-salt precipitates. These salts include villiaumite (NaF), kogarkoite (Na₃FSO₄), and natrophosphate (Na₇F(PO₄)₂·19H₂O).^{1,2,3} Fluoride produces melter off-gas that creates corrosion risk in the off-gas system piping, while the sulfate and phosphate in the fluoride double salts kogarkoite and natrophosphate can be detrimental to glass waste loading.⁴

Fluoride salts are sparingly soluble, with solubilities ranging from approximately 40 to 130 kg per kL of water.⁵ Even at equilibrium with water solvent, where the common ion effect is not a limitation as it is for supernatant solvent, a much larger volume of solvent is needed for dissolution than would be needed for a soluble salt such as sodium nitrate. The solubility per volume solvent is even lower when the solvent is a supernatant already containing dissolved sodium salts. The solubilities of the three fluoride salts are reasonably well known, and can be modeled using thermodynamic simulators, with some uncertainty. An overestimate of solubility means using more water and more storage space (or volume reduction) than planned. An underestimate of solubility means a higher concentration of fluoride, and possibly phosphate and sulfate, than planned for, which could produce corrosion or glass waste loading issues.

In contrast to solubilities, the dissolution kinetics of the three fluoride salts are not well known. There is little information on how rapidly equilibrium is approached and whether, for the double salts, the dissolution is stoichiometric during the dissolution transient. Unexpected delays in a tank dissolution process could be encountered as a result of the lack of information about dissolution rates. In addition, if the double salts show transient non-stoichiometric dissolution of fluoride versus phosphate or sulfate, unexpectedly high concentrations of one of the other constituents could be produced, with similar possible consequences for corrosion or HLW glass waste loading.

In an effort to mitigate future operations risk and to mature flowsheet technical bases, Washington River Protection Solutions authorized Pacific Northwest National Laboratory, to collect the available data for fluoride salt dissolution rate, provide a scoping estimate of dissolution time if possible, and identify gaps in the understanding and predictive capability for estimating dissolution time. Open literature and

¹ Herting DL, GA Cooke, and RW Warrant. 2002. *Identification of Solid Phases in Saltcake from Hanford Site Waste Tanks*. HNF-11585, Rev. 0, Fluor Hanford, Richland, Washington.

² Herting DL, GA Cooke, JS Page, and JL Valerio. 2015. *Hanford Tank Waste Particle Atlas*. LAB-RPT-15-00005, Rev. 0, Washington River Protection Solutions, Richland, Washington.

³ Reynolds JG, GA Cooke, DL Herting, and RW Warrant. 2013. "Salt mineralogy of Hanford high-level nuclear waste staged for treatment," *Ind. Eng. Chem. Res.*, **52**(29): 9741-9751, ACS Publications, Washington, D.C.

⁴ Tilanus SN, LM Bergman, RO Lokken, AJ Schubick, EB West, RT Jasper, SL Orcutt, TM Holh, AN Praga, MN Wells, KW Burnett, CS Smalley, JK Bernards, SD Reaksecker, and TL Waldo. 2017. *River Protection Project System Plan*, ORP-11242 Rev. 8, Office of River Protection, Richland, Washington.

⁵ Britton MD. 2019. *Solubility Data Review*, RPP-RPT-60326 Rev. 3, Washington River Protection Solutions LLC, Richland, Washington.

Hanford reports⁶ were reviewed to document, understand, and (where possible) evaluate limitations on fluoride salt equilibria and dissolution kinetics, including both mass transport and surface reaction rate. These reported tests used stepwise dissolution carried out under high-sodium conditions, which do not represent all the possible dissolution conditions, and did not assess whether equilibrium had been reached at the end of each step before adding more solvent. Dissolution times, intended to be useful at low precision – distinguishing between dissolution scenarios requiring hours versus days versus weeks of time – were estimated for one particular mechanism: mass-transfer-controlled dissolution of spherical particles of fluoride salts suspended in liquid. This is not the only governing mechanism; dissolution could be substantially slower if the surface reaction rate (the rate of release of ions from the surface) is the controlling mechanism.

When the minimum amount of water for complete dissolution is used and the slip velocity between the liquid and suspended particles is less than or equal to the terminal settling velocity, the estimated mass-transfer rates allow 100- μm particles of fluoride salt to dissolve in minutes at 25 °C in water containing no other dissolved salts. Much larger solids, such as the 6-mm particles or chunks that have been seen for natriphosphate heels, could take a few hours to more than a week to dissolve. The actual dissolution times will depend strongly on the actual slip velocity, the extent of particle suspension, the possible constraint by surface reaction rates (e.g., trace-metal inhibition of reaction), the ratio of solvent to solid, and the presence of common ions that shift the solubility equilibria to restrict the dissolution of fluoride salts.

Based on this study, the following recommendations are made:

- Further exercise the mass-transfer-controlled dissolution rate model developed in this study to approximate the effects of common ions, polydispersity of particle sizes, and higher slip velocities. A thermodynamic solubility model might provide predictions of the effective solubility of the fluoride salts in the presence of common ions, but is not necessary for low-precision estimates of dissolution time.
- Conduct laboratory studies of fluoride salt dissolution rates in simulants under conditions that can account for the effects of common ions, trace metals, and changes in solid surface area. The test apparatus and design must also allow the estimation of mass-transfer coefficients such that the effect of surface reaction rate can be distinguished from that of mass-transfer. This distinction is essential to being able to scale results to the various possible flow conditions in a tank dissolution process. For fluoride double salts, dissolution measurements should include both of the anions so that transient non-stoichiometric dissolution can be detected.
- Fill out the dataset for kogarkoite solubility with more testing. The dataset for kogarkoite solubility suggests that temperature has little effect on its solubility, but the data are sparse compared to those for the other two fluoride salts.

⁶ No Savannah River National Laboratory reports on fluoride-salt waste dissolution were found.

Acknowledgments

The authors thank Jacob Reynolds of Washington River Protection Solutions for technical feedback and funding for this work, and Michael Britton of Washington River Protection Solutions for supplying copious technical information. In addition, the authors thank Richard Daniel for his extensive technical reviews, Bill Dey for his thorough QA review and support, and Matt Wilburn for his technical editing. Thanks also to Chrissy Charron and Veronica Perez for their absolutely essential help with the project records.

Acronyms and Abbreviations

DFHLW	Direct Feed High-Level Waste
DST	double-shell tank
FA	fluorapatite
HA	hydroxyapatite
HLW	high-level waste
LAW	low-activity waste
ODE	ordinary differential equation
PNNL	Pacific Northwest National Laboratory
QA	quality assurance
R&D	research and development
SST	single-shell tank
WRPS	Washington River Protection Solutions
WTP	Waste Treatment and Immobilization Plant
WWFTP	WRPS Waste Form Testing Program

Contents

Summary	ii
Acknowledgments.....	iv
Acronyms and Abbreviations	v
Contents	vi
1.0 Introduction.....	1
2.0 Quality Assurance.....	3
3.0 Process Context.....	4
4.0 Fluoride Compounds in Waste.....	7
5.0 Solubility Equilibria.....	8
5.1 Solubility – Natrophosphate	8
5.2 Solubility – Kogarkoite.....	13
5.3 Solubility – Villiaumite	16
5.4 Solubility – Conclusions	19
6.0 Dissolution Rate – Observations on Hanford Waste	20
6.1 Stepwise Dissolution Tests	20
6.2 Other Observations on Hanford Waste	22
7.0 Dissolution Rate.....	23
7.1 Single-Salt Dissolution Rate – Limited by Mass Transfer	23
7.2 Single-Salt Dissolution Rate – Limited by Surface Reaction	29
7.3 Double-Salt Dissolution Rates – Theory	32
8.0 Observations, Conclusions, Gaps, and Recommendations	34
9.0 References.....	38

Figures

Figure 1. Concentration-Product $c_{FCPO_4}^2$ from Data for Natrophosphate $[Na_7F(PO_4)_2 \cdot 19H_2O]$ Equilibrium	11
Figure 2. Fluoride Concentration from Data for Natrophosphate $[Na_7F(PO_4)_2 \cdot 19H_2O]$ Equilibrium	12
Figure 3. Concentration-Product $c_{FC_{SO_4}}$ from Data for Kogarkoite (Na_3FSO_4) Equilibrium	15
Figure 4. Fluoride Concentration c_F from Data for Villiaumite (NaF) Equilibrium.....	18
Figure 5. Mass-Transfer Dissolution Time as a Function of Particle Size and Slip Velocity.....	31

Tables

Table 1. Inputs for Order-of-Magnitude Modeling of Mass-Transport-Controlled Dissolution	27
Table 2. Predictions from Order-of-Magnitude Modeling of Mass-Transport-Controlled Dissolution	27
Table 3. Measured Surface Reaction Constants or Dissolution Rates for Sodium Chloride in Water (Alkattan et al. 1997).....	30

1.0 Introduction

The Direct Feed High-Level Waste (DFHLW) flowsheet needs some level of leaching, washing, and solids concentration, which could occur in a new facility or potentially in double-shell tanks (DSTs). One species requiring leaching is fluoride, predominantly present as fluoride salt precipitates. These salts include villiaumite (NaF), kogarkoite (Na_3FSO_4), and natrophosphate [$\text{Na}_7\text{F}(\text{PO}_4)_2 \cdot 19\text{H}_2\text{O}$] (Herting et al. 2002, 2015; Reynolds et al 2013). Fluoride produces melter off-gas that creates corrosion risk in the off-gas system piping, while the sulfate and phosphate in the fluoride double salts kogarkoite and natrophosphate can be detrimental to glass waste loading (Tilanus et al 2017).

Fluoride salts are sparingly soluble, with solubilities ranging from approximately 40 to 130 kg per kL of water (Britton 2019). Even at equilibrium with water solvent, where the common ion effect is not a limitation as it is for supernatant solvent, a much larger volume of solvent is needed for dissolution than would be needed for a soluble salt such as sodium nitrate. It follows that large volumes of dissolution product are generated, requiring downstream volume reduction. Increasing the process temperature increases the solubility, particularly for natrophosphate, but adds to the complexity of dissolution operations and increases the risk of re-precipitation if process streams cool in downstream liquid handling.

In addition to solubility limits, there may be kinetic constraints on the rate of dissolution. Both kogarkoite and natrophosphate can form extremely large particles, millimeters to centimeters in diameter (Bolling et al. 2020; Reynolds and Herting 2016), suggesting that they may be kinetically slow to dissolve. It may be possible to increase the rate of dissolution by using an excess of solvent, but at the price of volume generation. Thus, the dissolution of fluoride salts may require a large amount of water for both equilibrium and kinetic reasons.

Because of these considerations, the dissolution equilibria and kinetics of the fluoride compounds are of interest. The intent of this report is to provide current knowledge of fluoride salt solubility and dissolution rate and to summarize the significance of the gaps in that knowledge.

Open literature and Hanford reports were reviewed to understand and, where possible, evaluate the following:

- The extent to which dissolution might be controlled by mass transfer versus being controlled by the rate of release of ions from the waste surface
- The dependence of transport-controlled dissolution on particle size, local flow rate, and diffusion coefficients
- Any evidence of the slowing of in-tank dissolution during tank retrievals that might indicate the formation of a shielding layer of insoluble residue on the surface, or other limitation on waste dissolution
- Information on double salt dissolution features, possibly drawing on non-sodium or non-fluoride double salts – including solubility equilibria, the effect of competing equilibria, transient incongruity during dissolution of congruent salts, and effects of trace metals on surface kinetics
- Hanford and Savannah River data related to equilibria and dissolution rates

Dissolution times intended to be useful at low precision – distinguishing between dissolution scenarios requiring hours versus days versus weeks of time – were estimated for mass-transport-controlled dissolution of spherical particles of fluoride salts suspended in liquid.

This report discusses the topics of dissolution processes that might be used (Section 3.0), the forms in which fluoride salts appear (Section 4.0), the solubility equilibria (Section 5.0), dissolution observations for Hanford waste (Section 6.0), and mass-transport and surface kinetics information from open literature (Section 7.0). Section 8.0 discusses conclusions that can be drawn and gaps in the available information with recommendations to close these identified technical gaps.

2.0 Quality Assurance

This work was conducted with funding from Washington River Protection Solutions (WRPS) under Pacific Northwest National Laboratory (PNNL) Project 75807, contract 36437-301, with the title “Flowsheet Maturation Studies.”

All research and development (R&D) work at PNNL is performed in accordance with PNNL’s Laboratory-level Quality Management Program, which is based on a graded application of NQA-1-2000, *Quality Assurance Requirements for Nuclear Facility Applications*, to R&D activities. To ensure that all client quality assurance (QA) expectations were addressed, the QA controls of the WRPS Waste Form Testing Program (WWFTP) QA program were also implemented for this work. The WWFTP QA program implements the requirements of NQA-1-2008, *Quality Assurance Requirements for Nuclear Facility Applications*, and NQA-1a-2009, *Addenda to ASME NQA-1-2008*, and consists of the WWFTP Quality Assurance Plan (QA-WWFTP-001) and associated procedures that provide detailed instructions for implementing NQA-1 requirements for R&D work.

The work described in this report was assigned the technology level “Applied Research” and was planned, performed, documented, and reported in accordance with procedure QA-NSLW-1102, *Scientific Investigation for Applied Research*. All staff members contributing to the work received appropriate technical and QA training prior to performing quality-affecting work.

3.0 Process Context

The DFHLW strategy represents one alternative flowsheet seeking to bypass the Hanford Waste Treatment and Immobilization Plant (WTP) Pretreatment Facility while retaining some key processing functions oriented towards maximum waste feed loading and minimization of high-level waste (HLW) volume. In addition to the baseline single-shell tank (SST) retrievals and waste transfers to DSTs, the DFHLW flowsheet needs some level of leaching, washing, and solids concentration, which could occur in a new facility or potentially in DSTs. At this time, these baseline DFHLW operations and facility capabilities have not been defined.

Fluoride can contribute substantially to the amount of solvent needed for dissolution, and the amount of liquid generated. Reynolds and Belsher (2017) give the example of tank AW-103, where the dominant salt is villiaumite (NaF) containing 115,000 kg of fluoride. They estimate that, in addition to the water volume required to wash out the sodium inventory in the interstitial liquid, 6,140,000 kg of water will be required to dissolve the villiaumite at equilibrium. Kinetic limitations on reaching equilibrium could make even more water necessary to achieve effective dissolution rates.

This study directly relates to potential HLW sludge washing operations and seeks to better understand and predict the rate and extent of fluoride salt dissolution to maximize HLW loading for fluoride-limited wastes. The effectiveness of sludge washing will be dependent on multiple process options selected in support of DFHLW. Each process option has varying advantages and disadvantages that will not be discussed here. Although not an exhaustive list, the key process options that affect sludge washing operations are summarized below and are presented to provide operational context around the dissolution of fluoride-containing salts in Hanford tank waste.

- **Potential washing fluids:** inhibited water (0.01 M NaOH and 0.011 M NaNO₂ [Uytioco 2015]), filtered river water, deionized water, dilute supernatant, and/or some as yet unspecified solvent
- **Potential washing fluid contact methods:** soaking, jet mixing, mechanical mixing, in-line mixing, and/or recirculation
- **Potential dissolution temperature ranges:** ambient waste temp (15 to 65 °C)⁷, heated washing fluid, heated waste by mechanical energy, and/or purpose-built heating
- **Potential washing operations variables:** diluent introduction location, total diluent volume, number of washes, diluent introduction rate, and/or mix/soak duration
- **Potential washing infrastructure:** DSTs, in transfer line, and/or new facility with purpose-built tanks that have heating/cooling capabilities and ideal geometry for mobilizing and mixing sludge solids
- **Potential materials of construction:** carbon steel, stainless steel, and/or other material suited specifically to handle erosion and corrosion

Clearly, many potential sludge washing operations options exist and need to be considered when establishing a strategy to effectively dissolve fluoride salts. However, past operational experiences and existing infrastructure do provide additional context on more likely approaches to be used at Hanford.

⁷ Upper temperature estimated based on the maximum waste feed acceptance criterion for HLW feed in 24590-WTP-ICD-MG-01-019, Rev. 7, 2014, *ICD-19 – Interface Control Document for Waste Feed*, Bechtel National, Inc., Richland, Washington.

Most if not all of the easily soluble or already dissolved salts (NaOH, NaNO₂, NaNO₃, and NaCl) will be at least partly removed from the solids during SST retrieval and transfer to DSTs. To remove the semi-soluble salts (Na₂CO₃ and Na₂SO₄) and the low solubility fluoride salts, it will probably be necessary to use filtered river water. The use of any solution containing sodium would be counterproductive due to the limited solubility (common-ion effect) and potential reduced mass transfer driving force for these sodium salts. More generally, saltcake retrieval is done primarily with filtered river water, whereas retrieval of sludge tanks is modeled with dilute supernatants in the DST system. For SST heel retrievals, sometimes 19 M NaOH or oxalic acid is added to dissolve heel solids consisting primarily of aluminum or iron, respectively.

One common approach to washing soluble components from sludge solids is to suspend the solids in the washing solution, let them settle, decant, and repeat. The stepwise method of contacting the solids with washing fluid improves the effectiveness of dissolution, relative to a single batch contact, by maintaining a concentration gradient to drive mass transfer with fresh wash solution. In a new purpose-built facility, though not in a mixing system added to an existing DST, the solids suspension system would be designed to fluidize any particle that could be transferred into the washing tank from the DSTs. Also, the solids suspension system would likely be designed to suspend the solids into a nearly homogeneous slurry for more efficient inter-tank transfers. If the kinetics of dissolution are slow, operations may mix for short periods limited by mechanical limits or heat, and then settle to decant the wash liquor.

If a high percentage of the fluoride needs to be removed, adding a heating system would be considered in preference to building additional tankage to perform more washing steps. Adding a heat source to an existing DST would be challenging, but this could be implemented in a purpose-built tank. Opportunistic heating could occur because of mechanical heat from jet mixer pumps or recirculation pumps.

Although more capital-intensive and involving higher operating costs, a purpose-built facility would be ideal since it would have design capabilities specific to sludge washing; however, washing could occur in the DST system. For example, AP-101, AP-102, AP-103, and AP-104 are informally designated DFHLW DSTs and are located in the north of AP Farm. This DFHLW 4-tank pack is co-located with direct feed low-activity waste operations DSTs AP-105, AP-106, AP-107 and AP-108 (south AP Farm). Both 4-tank sets are the closest DSTs to WTP, thus minimizing transfer line length. Furthermore, the service age and condition of the AP Tank Farm, and the fact that transfer lines tied to WTP originate from the AP-102 pump pit, are additional considerations making these north AP DSTs attractive to support the DFHLW mission phase.

Typically, dilute supernatant liquid is used to transport sludge solids to the north AP tanks. If washing is necessary, one potential option – an option that increases waste volume – is to transfer sludge to the north AP DSTs with filtered river water instead of supernatant liquid to opportunistically remove low-solubility salts during the mobilization and transfer of sludge solids.

The first steps of washing with water will displace/dilute the saltcake liquor. Once the existing saltcake liquor is displaced, the new saltcake liquor will probably have low concentrations of OH⁻, NO₃⁻, and NO₂⁻, making it more corrosive to the carbon steel DSTs. Further dissolution will likely need to be in newly constructed tank(s) composed of materials that will not corrode in a solution with high fluoride and low hydroxide, nitrate, and nitrite.

Many process operations exist for dissolving fluoride salts in tank waste, but the best strategy has not yet been defined and documented. The effectiveness of fluoride-salt dissolution is closely tied to the operational considerations briefly discussed above. This operational context and its applicability to the success of fluoride-salt dissolution is important to maintain in reference to discussions in the rest of this report, which seeks to establish the bases for predicting fluoride-salt dissolution rates and extent. This

information serves as an initial approach to making these difficult and potentially expensive operations and facility choices for DFHLW.

4.0 Fluoride Compounds in Waste

Several fluoride compounds have been observed in tank waste or are known to have been present at one time. Some of these are sludge minerals, rather than salts. Cryolite (sodium aluminum fluoride, Na_3AlF_6), has been seen in solids from BY-109 and C-107 (Herting et al. 2015). It is not soluble in water. Fluorozirconates and fluorosilicates were present in cladding waste before it was fully neutralized, but as yet have not been seen in current fully-neutralized tank waste because they undergo hydrolysis at high pH (Herting et al. 2015).

The remaining three fluoride compounds are sodium salts, which are of significance in the present study: the single salt villiaumite (sodium fluoride, NaF), the double salt natrophosphate (sodium fluoride phosphate, $\text{Na}_7\text{F}(\text{PO}_4)_2 \cdot 19\text{H}_2\text{O}$), and the double salt kogarkoite (sodium fluoride sulfate, Na_3FSO_4). All three of these salts can co-exist in the solid phase, if there is enough fluoride.

Villiaumite forms octahedral crystals (Herting et al. 2002). As of 2011, the maximum primary particle size was considered to be less than 20 μm (Wells et al. 2011). However, in a later study primary crystals of up to 50 μm size were found in water-leached waste from AW-105 (Huber 2013).

Natrophosphate forms compact octahedral and cuboctahedral primary crystals (Herting et al. 2002) with an observed maximum size in the range of 2000 μm (Wells et al. 2011). Core-sampled solids from AP-103 and AP-108 contained natrophosphate crystals ranging from 10 μm to greater than 1000 μm in size (Reynolds et al. 2013). In the AP-103 core samples, natrophosphate was the most prevalent salt. Some coarse, blocky aggregates (as large as 5000 μm) have also been seen in grab samples of AP-107 waste (Bolling et al. 2017; Bolling et al. 2020). In these samples, roughly one-third of the solid material was made up of coarse material (larger than 425 μm sieve size), which appeared to be fragments of larger crystals, with the remainder being relatively fine particles with sizes in the range of 25 to 100 μm . Even larger particles and aggregates of natrophosphate were found in the waste heel in tank C-108 (Callaway and Huber 2010), sometimes in conjunction with trona. The natrophosphate/trona combination was found in samples that were partly taken from a hard layer at the bottom of the tank. About 20 wt% of the coarsest “pebbles” would not pass through a 1/4-inch (~6 mm) sieve.

Natrophosphate is a congruent salt (Herting et al. 2002), meaning that when water is added to the pure salt, the $\text{Na}:\text{F}:\text{PO}_4$ ratios will be the same in the liquid (when it reaches equilibrium) as in the salt solid. This salt has been demonstrated to be a true double salt, rather than a solid solution with varying ratios on constituents (Herting and Reynolds 2016).

Kogarkoite is also a congruent salt (Herting et al. 2002). Its crystals have most often been observed in the form of hexagonal plates (Herting et al. 2015), though an acicular (needle-shaped) crystal form has been seen in grab samples of AP-107 waste (Bolling et al. 2020) and core samples from AP-103 and AP-108 (Reynolds et al. 2013). The range of coarse and fine particle sizes in the AP-107 samples was roughly the same for kogarkoite as for natrophosphate. There was no evidence that chloride had substituted for fluoride in the crystal structure. The acicular kogarkoite particles in AP-103 solids formed radial aggregates resembling balls of needles.

It may be worth noting that the fluoride salt aggregates in the AP-107 waste exhibited self-aggregation (Bolling et al. 2017; Bolling et al. 2020). That is, natrophosphate [$\text{Na}_7\text{F}(\text{PO}_4)_2 \cdot 19\text{H}_2\text{O}$] and kogarkoite (Na_3FSO_4) were not found together in any aggregate, but were always found separately.

5.0 Solubility Equilibria

The equilibrium solubilities of salts determine the maximum amount of fluoride that can enter solution (at the potentially long time required to closely approach equilibrium). The common-ion effect of anions will cause solubility of the fluoride double salts to be inhibited by the presence of other salts, single or double, that contain phosphate or sulfate. Sodium salts of phosphate and sulfate are, in Hanford waste, the most plausible inhibitors through the common-anion effect. These include $\text{Na}_3\text{PO}_4 \cdot 0.25\text{NaOH} \cdot 12\text{H}_2\text{O}$, Na_2SO_4 , and double salts of sulfate such as $\text{Na}_6\text{CO}_3(\text{SO}_4)_2$ and $\text{Na}_3\text{NO}_3\text{SO}_4 \cdot \text{H}_2\text{O}$.

Another type of decrease in fluoride salt solubility applies to both single and double fluoride salts. This decrease is caused by sodium salts such as sodium nitrate (often present in high concentration in waste liquids). These other sodium salts inhibit dissolution of sodium fluoride salts through the common-cation effect of their soluble Na content. The highly soluble sodium salts such as sodium nitrate must be washed away before fluoride salts can dissolve to any appreciable extent.

In a separate effect, increasing the ionic strength of the liquid (increasing concentration of sodium and its counterions) decreases the activity of water. This change in water activity somewhat increases the solubility of salts that incorporate waters of hydration, such as natrophosphate.

Finally, the fact that phosphoric acid is a weak acid means that pH may play a part in natrophosphate salt solubility. The pKa values (acid dissociation constants) for phosphoric acid are 12.1 for PO_4^{-3} vs. HPO_4^{-2} , 7.2 for HPO_4^{-2} vs. $\text{H}_2\text{PO}_4^{-1}$, and 2.1 for $\text{H}_2\text{PO}_4^{-1}$ vs. H_3PO_4 (CRC 1975). As a result, at a pH of 12 – which is the nominal pH for inhibited water at 0.01 M NaOH / 0.011 M NaNO_2 (Uytioco 2015) that is sometimes used at Hanford – part of the phosphate that dissolves from natrophosphate will be in the form of PO_4^{-3} and part in the protonated HPO_4^{-2} . This protonation allows for a higher fluoride concentration in equilibrium with the remaining unprotonated PO_4^{-3} concentration from dissolved salt. Hydrofluoric acid and sulfuric acid have much lower pKa values, so their dissociation is unlikely to have much effect on fluoride salt solubility at the alkaline conditions that are present in Hanford waste, even when it is diluted.

5.1 Solubility – Natrophosphate

The solubility expression for natrophosphate [$(\text{Na}_7\text{F}(\text{PO}_4)_2 \cdot 19\text{H}_2\text{O})$] is

$$c_{\text{Na}}^7 c_{\text{F}} c_{\text{PO}_4}^2 c_{\text{H}_2\text{O}}^{19} = \frac{K_{\text{NFP}}}{\gamma_{\text{Na}}^7 \gamma_{\text{F}} \gamma_{\text{PO}_4}^2 \gamma_{\text{H}_2\text{O}}^{19}} \quad (1)$$

where c_i is the molal concentration (mol/kg water in solution) of species i , γ_i is the activity coefficient of species i at the solution composition and temperature, and K_{NFP} is the solubility constant of natrophosphate at the solution temperature. By definition, the molal concentration of water is a constant (55.5 mol/kg water).

In Eq. (1), the solubility product is expressed in terms of species activities, the appropriate form in cases where there are high concentrations and multiple ions present. Each species activity is the product of its concentration and its activity coefficient. Eq. (1) separates the concentrations and coefficients to lie on different sides of the equation, so that the directly observable concentration product is shown in terms of the thermodynamic parameters. The solubility product is a function of temperature but not concentration. The activity coefficients are functions of both temperature and interactions with every species that is present, with each species potentially having a different effect based on its concentration, charge, and other properties. The common-ion effects are driven predominantly by the left-hand side of the equation and the exponents to which concentrations are raised, though activity coefficients also play a part. For

natrophosphate, the common-ion effect of sodium is very strong because sodium concentration is raised to an exponent of 7.

Figure 1 shows the directly observable product $c_F c_{PO_4}^2$ as a function of c_{Na} for experimental data. The data with black and red symbols come from simple solutions that have no co-anions (only Na^+ , F^- , and PO_4^{3-}) or one or two co-anions (either NO_3^- or a combination of NO_3^- and OH^-). The black symbols are for data taken at 25 °C, the red for data at 50 °C. These simple-solution data are a subset from the spreadsheet database developed by Britton (2019).⁸ The subset included only those tests where warning flags were absent,⁹ natrophosphate solid was observed,¹⁰ and dissolved sodium concentration was less than 9 m Na (representing diluted concentrations in retrieved Hanford waste). No co-anion solids ($NaNO_3$, for one possible example) were observed in the plotted data subset.

Figure 1 also indicates where a fluoride or phosphate solid other than natrophosphate was present in equilibrium with the simple solutions. At fluoride concentrations high enough to allow sodium fluoride (NaF) to be observed along with natrophosphate, a thin black circle is drawn around the data point. A thin black square is used to indicate the presence of $Na_3PO_4 \cdot 0.25NaOH \cdot 12H_2O$ with natrophosphate, at high phosphate concentration. The presence of sodium fluoride is a sign of a low ratio of PO_4^{3-}/F^- , whereas the presence of $Na_3PO_4 \cdot 0.25NaOH \cdot 12H_2O$ is a sign of a high ratio.

The data with green symbols, in Figure 1, are a subset of data found in a number of laboratory studies of stepwise dissolution of Hanford tank wastes at 25 °C (Herting and Edmonson 1998; Herting 1999, 2000, 2001, 2002; Herting and Bechtold 2002; Callaway 2003). In a stepwise dissolution test, water (or another solvent) is added to a waste sample and mixed for roughly 24 h. Then the excess liquid is separated from the remaining solids, and another increment of solvent is added to the solids to continue the dissolution.¹¹

Note that the waste dissolution studies (unlike the simple solution tests) did not include any direct observations of solid phases present during dissolution. The presence of natrophosphate [$Na_7F(PO_4)_2 \cdot 19H_2O$] was inferred from the behavior of F^- and PO_4^{3-} concentrations in the liquid – so long as both were increasing with each step of dissolution, some undissolved natrophosphate was considered to have still been present during the preceding dissolution step. Observations of solid phases present in the initial waste (before dissolution) were also used as evidence. Data for non-water solvents and data in which there was no definite evidence of the presence of natrophosphate solid were excluded from the subset.¹²

⁸ The database, which is consistent with the Britton (2019) report, was obtained from MD Britton in the form of a spreadsheet file, “RPP-RPT-60326-02, Reference Solubility Data-166.xlsm”. The provenance is documented in PNNL internal document TDP-OSIF-003 (not publicly available).

⁹ The “Status” entries used as a basis for exclusion were “Accepted, Duplicate”, “Duplicate”, “MSE Validation, Accepted, Duplicate”, “MSE Validation, Duplicate”, “MSE Validation, Outlier”, “MSE Validation, Rejected”, “No Conversion Equation”, “Not Original Data”, “Outlier”, “Outlier, Duplicate”, “Outlier, Metastable”, “Outlier, Regressed”, “Regressed”, “Rejected”, “Rejected, Duplicate”, or “Rejected, Regressed”. The “Solid Present – As Reported” entries used as a basis for exclusion were “Not Reported” or “Solids Reporting Error”.

¹⁰ Data were excluded when the observed solids did not include $Na_7F(PO_4)_2 \cdot 19H_2O$ (abbreviated as “NaFPO4”), or the combination of NaF and Na_3PO_4 . Only data for certain temperatures and co-anions are shown. In addition, a few data points were excluded because no fluoride concentration was given.

¹¹ A minority of the data were measured after substantially shorter mixing times, 5 to 90 min. These points are not distinguished in the plot.

¹² Other reasons for exclusion included a charge balance outside the range 0.85 to 1.15, or absence of measurements of hydroxide. High sodium concentration data were not excluded for the Hanford waste data, though they had been excluded from the simple solution data.

The following features of the concentration product $c_F c_{PO_4}^2$ at natrophosphate equilibrium can be seen in Figure 1:

- (a) When there is no co-anion – when only Na^+ , F^- , and PO_4^{3-} are present, shown by the “x” symbols at low Na concentration – the concentration product increases as the ratio of PO_4^{3-}/F^- increases. That ratio is not plotted, but can be recognized by the presence of sodium fluoride (NaF) at the lower end of the product range and $Na_3PO_4 \cdot 0.25NaOH \cdot 12H_2O$ at the upper end. The higher concentration products at high phosphate may be related to the PO_4^{3-} vs HPO_4^{2-} acid/base equilibrium already mentioned. The acid/base behavior of fluoride would have less of an effect than that of phosphate.
- (b) The concentration products found in the presence of NO_3^- co-anion (square symbols for data) show little difference between high-phosphate and high-fluoride conditions. Possibly the increased Na associated with the co-anion has decreased the solubility of natrophosphate enough to make the buffering acid/base behavior of phosphate less significant.
- (c) The concentration product decreases as Na increases because of the common-ion effect of the other Na salts (sodium nitrate and sodium hydroxide). However, the trend is not as strong as the inverse of c_{Na}^7 that would be expected from the left side of Eq. (1); this is the effect of changes on ion and water activities.
- (d) The simple-solution data for 25 °C and 50 °C show a concentration product that is at least a factor of 10 higher for the higher temperature.
- (e) Within the range of Na concentrations for which simple-solution data are plotted, the 25 °C waste dissolution concentration products are broadly in agreement with the 25 °C products from simple solutions. However, at about 1 to 3 m Na, there are some high-concentration products from the waste solutions. One possible explanation is that acid-base buffering increased the solubility. Another is that the “fluoride” measurement included not only fluoride but low-molecular-weight organic acid ions such as formate, giving an overestimate of $c_F c_{PO_4}^2$. Figure 2 shows the fluoride concentrations for the same data sets as Figure 1, plotted with the same conventions. The waste-dissolution fluoride concentrations frequently exceed the simple-solution concentrations.
- (f) At higher Na concentrations where only the waste dissolution data are plotted, there is substantial scatter in the concentration products, but it appears the trend of decreasing product with increasing Na is no longer present, and may even be reversed. The decrease in water activity already alluded to may be contributing to the change in trend.

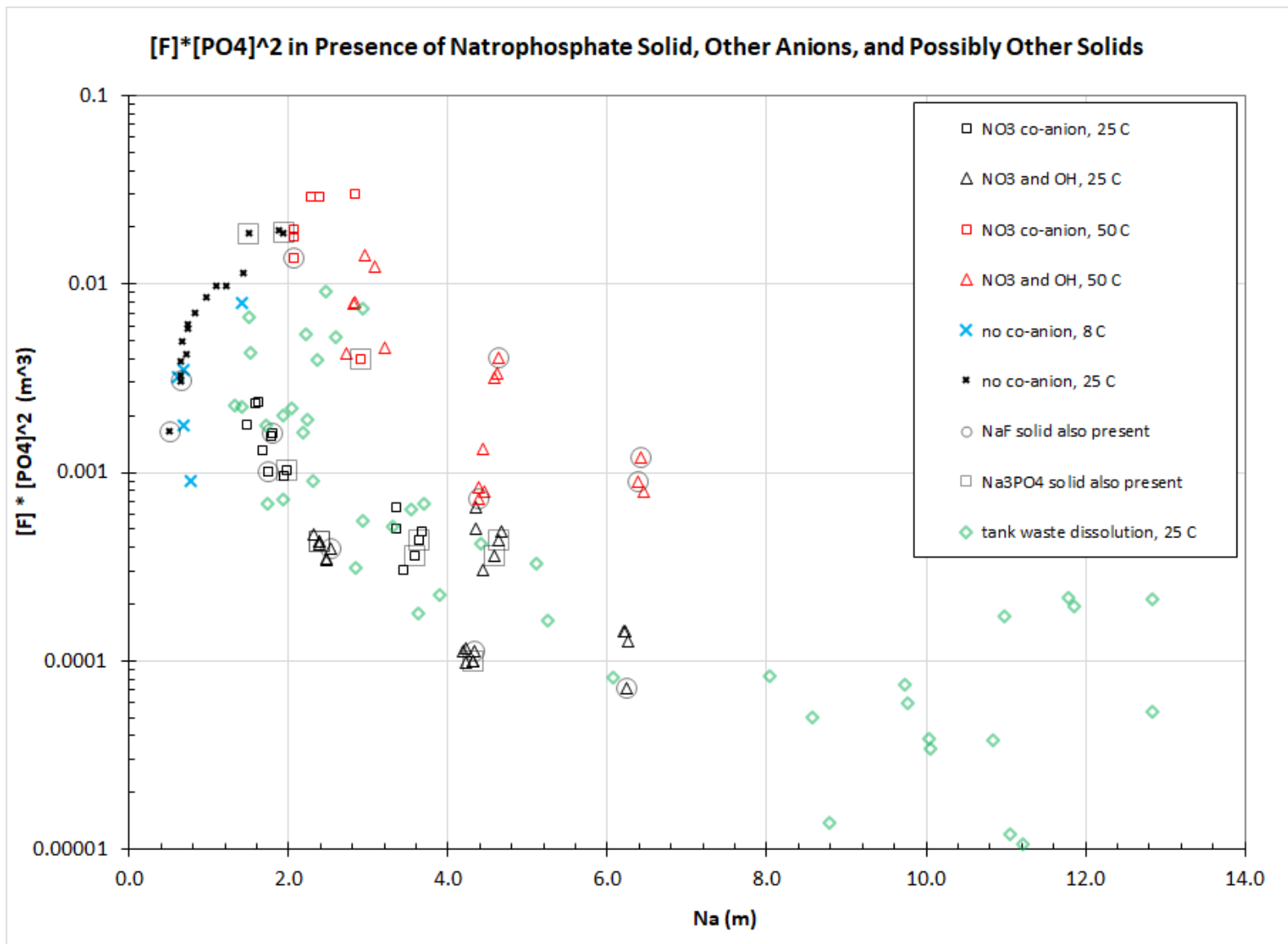


Figure 1. Concentration-Product $c_{FCPO_4^2}$ from Data for Natrophosphate $[Na_7F(PO_4)_2 \cdot 19H_2O]$ Equilibrium

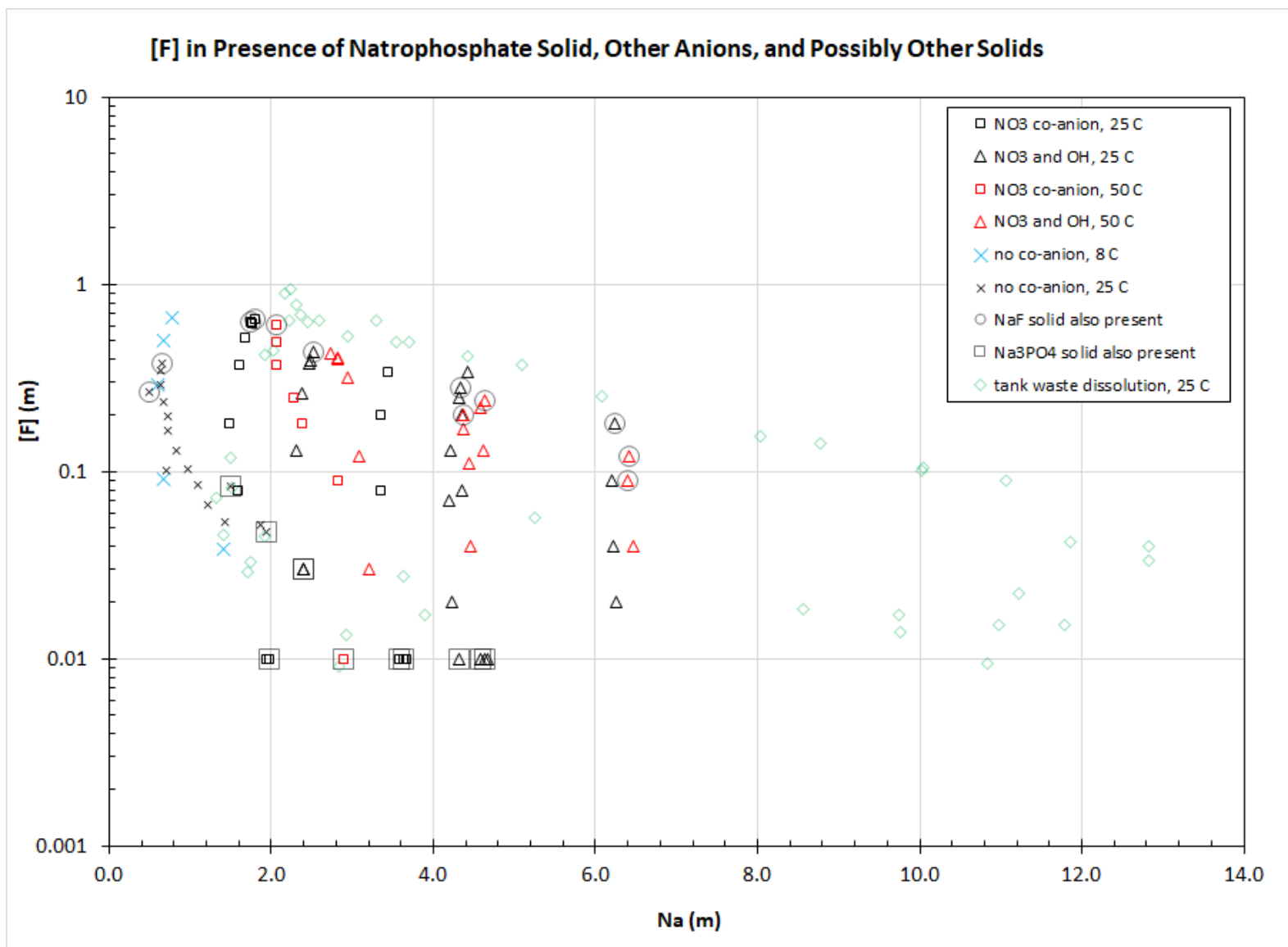


Figure 2. Fluoride Concentration from Data for Natrophosphate $[\text{Na}_7\text{F}(\text{PO}_4)_2 \cdot 19\text{H}_2\text{O}]$ Equilibrium

5.2 Solubility – Kogarkoite

The solubility expression for kogarkoite (Na_3FSO_4) is

$$c_{\text{Na}}^3 c_{\text{F}} c_{\text{SO}_4} = \frac{K_{\text{NFS}}}{\gamma_{\text{Na}}^3 \gamma_{\text{F}} \gamma_{\text{SO}_4}} \quad (2)$$

where K_{NFS} is the solubility constant of kogarkoite at the solution temperature.

Figure 3 shows the product $c_{\text{F}} c_{\text{SO}_4}$ as a function of c_{Na} for experimental data. The data with black and red symbols come from simple solutions that have either no co-anions (only Na^+ , F^- and SO_4^{2-}) or one co-anion, as listed in the legend. The black symbols are for data taken at 25 °C, the red for data at 50 °C. These simple-solution data were selected in much the same way as for natrophosphate, but with a focus on kogarkoite solids and anions.

Figure 3 also indicates the cases where a fluoride or sulfate solid other than kogarkoite was present in equilibrium with the simple solutions. At fluoride concentrations high enough to allow sodium fluoride to be observed along with kogarkoite, a thin black circle is drawn around the data point. A thin black square is used to indicate the presence of sodium sulfate with natrophosphate, at high sulfate concentration.¹³ The presence of sodium fluoride is a sign of a low ratio of $\text{SO}_4^{2-}/\text{F}^-$, whereas the presence of sodium sulfate is a sign of a high ratio. In some cases, a co-anion solid, NaCl, was observed in this data subset.

The data with green symbols, in Figure 3, are from stepwise waste dissolution data, as for preceding figures. The presence of kogarkoite was inferred from the behavior of F^- and SO_4^{2-} concentrations in the liquid. Observations of solid phases present in the initial waste (before dissolution) were also used as evidence. Data in which there was no definite evidence of equilibration with kogarkoite solid were excluded from the subset; other reasons for exclusion are the same as for natrophosphate.

The following features of the concentration product $c_{\text{F}} c_{\text{SO}_4}$ at kogarkoite equilibrium can be seen in Figure 3:

- When there is no co-anion – when only Na^+ , F^- and SO_4^{2-} are present, shown by the “×” symbols at low Na concentration – the concentration product does not show any dependence on the ratio of $\text{SO}_4^{2-}/\text{F}^-$, unlike the apparent dependence of natrophosphate solubility on the ratio of $\text{PO}_4^{3-}/\text{F}^-$. Since sulfuric acid is a strong acid, acid/base equilibrium would not affect kogarkoite dissolution.
- The concentration products found in the presence of co-anions also show no quantifiable difference between high-sulfate and high-fluoride conditions.
- The concentration product decreases as Na increases because of the common-ion effect of the other Na salts (sodium nitrate and sodium hydroxide). A trend proportional to the inverse of c_{Na}^3 would be expected from the left side of Eq. (2).
- The simple-solution data for 25 °C and 50 °C show concentration products that are not higher at the higher temperature, and may even be lower. For comparison, Toghiani et al. (2005), whose work supplied much of the simple-solution data in Figure 3, found a slight increase in NaF

¹³ There are some low-temperature data where Na_3FSO_4 was not listed as a solid, but rather a combination of NaF and $\text{Na}_2\text{SO}_4 \cdot n\text{H}_2\text{O}$. These appear in Figure 3 with a combination of thin black circles and thin black squares. It is hard to know how to interpret which combination of solid phases was actually present, but kogarkoite must have been among the solids.

solubility over this temperature range from 4.09 to 4.35 g NaF/100 g H₂O. The Na₂SO₄ solubility increased more strongly, from 28.0 to 46.3 g Na₂SO₄/100 g H₂O (Toghiani et al. 2005).

- (e) Within the range of Na concentrations for which simple-solution data are plotted in Figure 3, the 25 °C waste dissolution concentration products are broadly in agreement with the 25 °C products from simple solutions.
- (f) At higher Na concentrations where only the waste dissolution data are plotted, the trend of decreasing product with increasing Na appears to be the same as for the range of lower Na concentration. There is no obvious change in trend for this non-hydrated salt, which is unlike the behavior of natrophosphate (with its large number of waters of hydration).

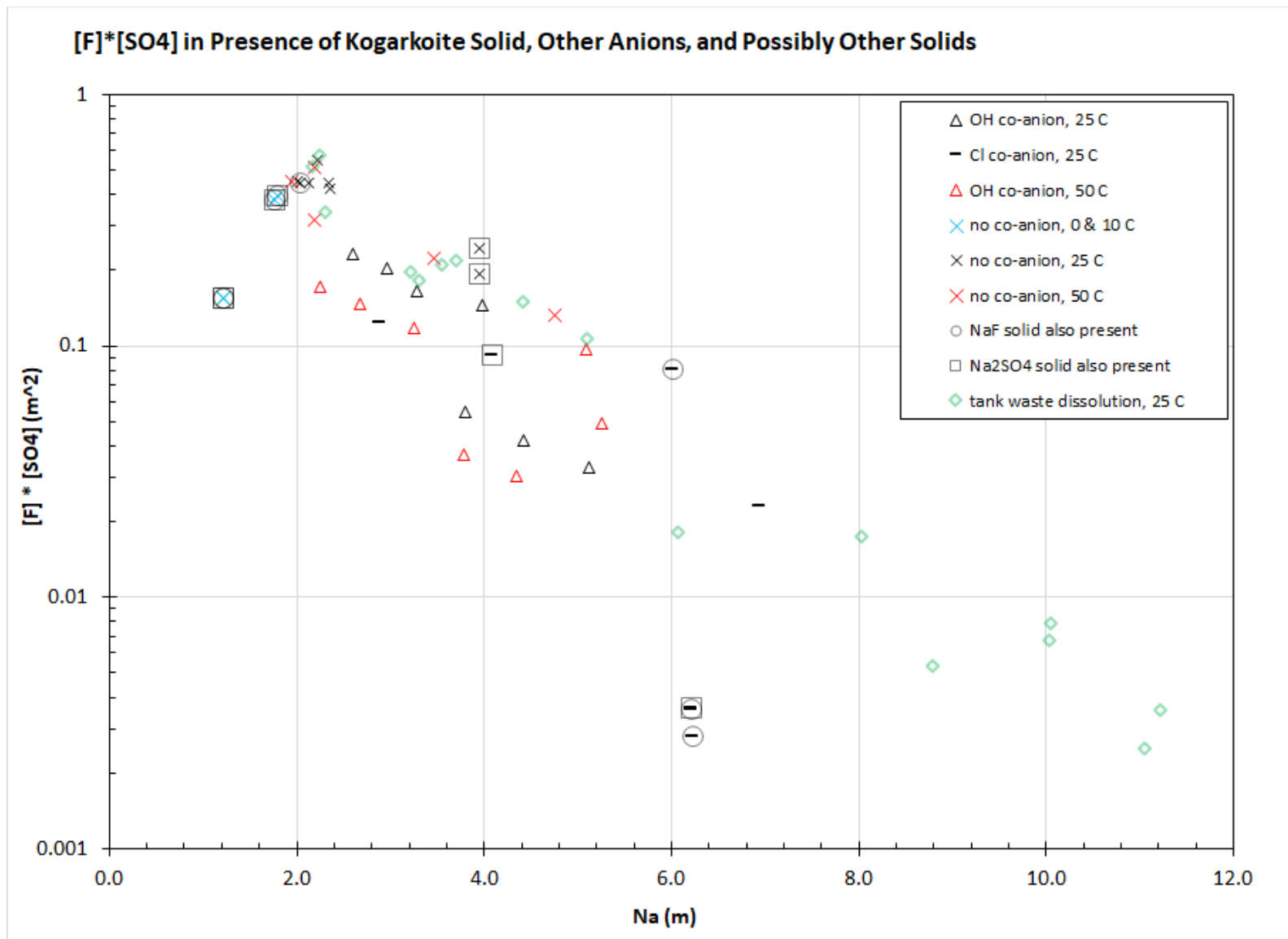


Figure 3. Concentration-Product $c_{FC_{SO4}}$ from Data for Kogarkoite (Na_3FSO_4) Equilibrium

5.3 Solubility – Villiaumite

The solubility expression for villiaumite (NaF) is

$$c_{Na}c_F = \frac{K_{NF}}{\gamma_{Na}\gamma_F} \quad (3)$$

where K_{NF} is the solubility constant of villiaumite (NaF) at the solution temperature.

Figure 4 shows the fluoride concentration c_F as a function of c_{Na} for experimental data. The data with black and red symbols come from simple solutions that have either no co-anions (only Na^+ and F^-) or one co-anion, as listed in the legend. Data where sulfate or phosphate were present in solution are not included, to avoid focusing on the double salt effects. The black symbols are for data taken at 25 °C, the red for data at 50 °C. These simple-solution data were selected in much the same way as for natrophosphate, but with a focus on villiaumite and fluoride. In some cases, a co-anion solid was observed in this data subset.

No data from stepwise waste dissolution are included in Figure 4. Villiaumite was almost certainly present in some of the wastes, but it is difficult to distinguish its effect on dissolved fluoride concentration from that of the fluoride double salts.

The following features of the fluoride concentration c_F at villiaumite equilibrium can be seen in Figure 4:

- (a) When there is no co-anion, fluoride appears to increase steeply, for each plotted temperature, over narrow ranges of increasing Na concentration near 1 m Na. This may be an artifact or an acid-base effect.
- (b) The fluoride concentrations found in the presence of co-anions decrease steeply with increasing Na in the range between 1 and about 1.5 m Na.
- (c) Above about 1.5 m Na, the fluoride concentration decreases as Na increases in a trend that seems to be close to the inverse of c_{Na} that would be expected from the left side of Eq. (3). However, this trend seems to be flattening out above 6 m Na, which would be consistent with discussion by Reynolds (2018) about the behavior of NaF solubility when NO_3^- is the co-anion.
- (d) The data where there are no co-anions show an increase in fluoride with temperature. Toghiani et al. (2005) found a slight increase in NaF solubility from 25 °C and 50 °C: from 4.09 to 4.35 g NaF/100 g H_2O , which corresponds to an increase of about 0.01 molal/°C. Another source (Reynolds and Belsher 2017) correlated NaF solubility versus temperature in the range from 0 to 100 °C, drawing on a number of literature sources of data, and estimated an increase in solubility of about 0.003 molal/°C. Reynolds and Belsher (2017) noted substantial scatter in the solubility data. However, the data for 25 °C and 50 °C when co-anions are present show fluoride concentrations that are not consistently higher at the higher temperature, when the two temperatures are compared for the same co-anion.
- (e) The identity of the co-anion would be expected to make some difference in the fluoride concentration at a given temperature and Na concentration, with solubility of NaF following the trend $\text{NaNO}_3 > \text{NaCl} > \text{NaOH}$ for the same sodium molality (Reynolds 2018). No clear trend of that kind is visible in the scattered data in Figure 4. However, the presence of CO_3^{2-} co-anion (“+” symbols) is frequently associated with relatively high fluoride concentration. Since carbonate was present in the absence of any added hydroxide, the acid/base behavior of carbonate may have

played a part. The pKa values for carbonic acid are 10.2 for CO_3^{-2} vs. HCO_3^{-1} and 6.4 for HCO_3^{-1} vs. H_2CO_2 (CRC 1975).

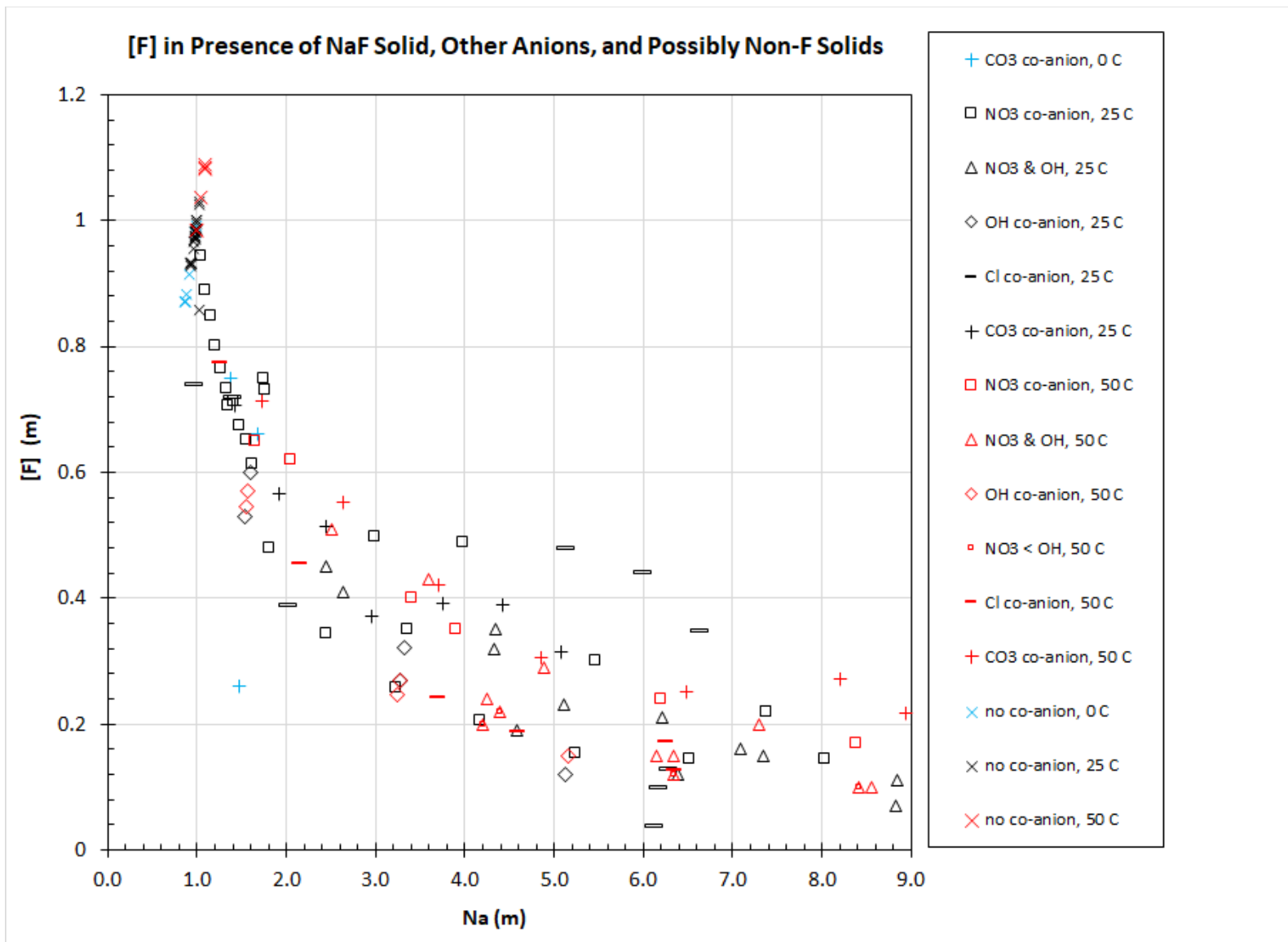


Figure 4. Fluoride Concentration c_F from Data for Villiaumite (NaF) Equilibrium

5.4 Solubility – Conclusions

The preceding discussion leads to the following conclusions:

- (a) When there are no co-anions – when water is the solvent – phosphate or fluoride acid/base behavior may increase the effective solubility of natrophosphate [$\text{Na}_7\text{F}(\text{PO}_4)_2 \cdot 19\text{H}_2\text{O}$] and villiaumite (NaF). Phosphate is the more plausible buffer for alkaline Hanford waste. The use of inhibited water (at 0.01 M NaOH and 0.011 M NaNO_2 [Uytioco 2015]) for dissolution might allow for this enhanced solubility, but more concentrated caustic would not.
- (b) The presence of carbonate as a buffer might hold pH at a level where the solubility of natrophosphate is increased.
- (c) The solubility decreases for all the fluoride salts as Na increases because of the common-ion effect of the other Na salts (sodium nitrate and sodium hydroxide). However, for natrophosphate, increasing the Na concentration above about 6 m Na may not cause a further decrease in the solubility; this is unclear because of scatter in the data.
- (d) The simple-solution data for 25 °C and 50 °C show that the concentration product for natrophosphate is at least a factor of 10 higher for the higher temperature, whether co-anions are present or not. However, when co-anions are present there is no clear effect of temperature on villiaumite, although an increase in solubility with temperature is seen when co-anions are absent. For kogarkoite (Na_3FSO_4), temperature has little effect in the absence of co-anions, and an increase in temperature may even decrease solubility when co-anions are present. However, data for kogarkoite are too sparse for a firm conclusion. The implication is that increasing the solvent temperature would provide an advantage in dissolving natrophosphate versus the other two fluoride salts.

The data presented above contain scatter both from measurement uncertainty (or error) and from species interactions that are not quantifiable from raw data alone. In general, the effects or implications discussed above can best be evaluated by using thermodynamic solubility models so that interactions can be systematically and consistently accounted-for by species activity calculations. This will tend to offset gaps in the raw data, although some of the scatter in the data will affect the predictions of thermodynamic models because their activity parameters are based on some of the same data.

6.0 Dissolution Rate – Observations on Hanford Waste

Several types of Hanford Site dissolution observations have been reviewed.¹⁴ Most observations have been made during stepwise dissolution tests, but a few observations from other types of tests are also available.

6.1 Stepwise Dissolution Tests

A number of tests of stepwise waste dissolution (also called “cascade” dissolution) have been carried out at ambient temperature (22 to 25 °C) by Herting and Edmonson (1998), Herting (1999, 2000, 2001, 2002), Herting and Bechtold (2002), and Callaway (2003), among others. In most of these studies, the minimum time between each diluent addition and the subsequent decant step was in the range of 20 to 24 h, varying a little between studies. The diluted samples were actively mixed, usually by initial vortex mixing followed by continuous end-over-end tumbling. There was no test of whether a longer mixing interval would produce higher concentrations (i.e., whether equilibrium had been reached). It seems likely that equilibrium was reached over these periods of 20 or more hours per step, but there is no information on how much less time would have been needed to reach equilibrium under those well-mixed conditions.

Two of these stepwise dissolution tests employed much shorter contact times. Herting (2000) measured radionuclide phase distribution with well-mixed 1-h contact times, followed by 30 min of centrifugation. The incremental additions of inhibited water (0.01 M NaOH and 0.01 M NaNO₂) were each 50% of the initial sample weight, with dissolution liquid decanted between steps. Wastes from tanks BY-106, S-102, and A-101 were tested, with chemical components measured as well as radionuclides. A shorter-contact test, intended to emulate dissolution by percolation through a column, was conducted for BY-102 waste by Herting (1999). Samples were mixed with increments of inhibited water for 5 min, then centrifuged for 30 min and decanted. The dilution increment was gradually increased from 33 wt% of the initial sample to 133 wt% over eight steps. Note that in these tests the centrifugation time was substantial compared to the nominal mixed contact time, so the effective contact time unavoidably has some uncertainty.

Note that 24-h contact dilutions were conducted by Herting and Edmonson (1998) for BY-102 and BY-106 wastes and by Herting (1999) for A-101 and S-102 wastes. It would be possible to compare the concentrations from the short-contact tests against those from nominally 24-h contact tests for the same tanks, with the caveat that the composition of the waste samples might be different, if compositing used different proportions of samples. That contact-time comparison has not been carried out in this report.

The S-112 waste-sample dissolution studies (Herting and Bechtold 2002) included kinetics-related surface dissolution tests. About 8 g of sample was put into a 30-mL vacuum funnel with a glass frit bottom. The sample surface sloped to allow water dripped from above to run down the surface into an area of the funnel bottom that was not covered by the sample. Some channeling occurred, although the location of the water addition point was changed periodically. Most of the water ran into the solid, rather than down the sloped surface. The total added dilution water amounted to about 110% of the sample by weight.

Herting and Bechtold (2002) conducted the surface dissolution tests with water addition times of 30 s, 2 min, 5 min, 23 min, and 60 min. The actual water contact time was not quantified; it was described as being much shorter than the water addition time, and as tending to be relatively constant despite

¹⁴ Only Hanford references were reviewed. Savannah River National Laboratory was contacted to find more information on dissolution of salt wastes, but no reports were identified that discussed salt dissolution.

differences in the water addition time. Control samples were prepared to represent equilibration after a long contact time. For these cases, S-112 waste and water were mixed for 3 days, using dilution similar to that in the surface dissolution tests.

The S-112 test results are not directly applicable to fluoride salt dissolution because the S-112 waste had such low fluoride content that fluoride salts were not observed in the solid phase and dissolved fluoride was below detection in the liquid. However, it is interesting to note that NO_3^- had reached only about 50% of its 3-day equilibrated concentration after a 23-min water addition and only about 80% after a 60-min addition. Many other species showed similar behavior. A definite exception was PO_4^{3-} , which remained further from equilibrium: It was at about 40% of the equilibrated value after a 23-min water addition and about 50% after a 60-min addition.

One conclusion is that even a species with a high driving force for dissolution (high solubility), such as nitrate, did not reach equilibrium within a contact time of 1 h or less. Another is that $\text{Na}_3\text{PO}_4 \cdot 0.25\text{NaOH} \cdot 12\text{H}_2\text{O}$ salt, which was present in small amounts in the waste solids (Herting and Bechtold 2002), was limited in its dissolution rate. It is not clear whether this was because of a lower driving force (solubility) or a slower surface reaction to release the phosphate ion, or both.

On a related matter, part of the original scope of this report was to assess fluoride salt dissolution rates by finding retrieval conditions under which salt dissolution did not reach equilibrium. The intent was to use the data to evaluate mass-transfer limitations caused, e.g., by the salt surface being shielded by a layer of poorly-soluble solids that remained behind after the dissolution of more soluble salt. It was thought that reviewing tank retrieval data, and looking for decreases in the density of the retrieved liquid, might indicate situations where sodium nitrate dissolution was being limited by some such mass-transfer barrier. The liquid density is strongly dependent on the soluble major-constituent salt sodium nitrate, so density might serve as a surrogate for nitrate content, with subsaturated concentrations of nitrate being a surrogate for subsaturation of fluoride salts. However, the retrieval data were ambiguous because decreases in liquid density occurred together with process difficulties such as saltwell collapse. Therefore, the attempt to make inferences from retrieval data was abandoned.

There are four gaps in the waste dissolution data discussed in this section:

1. The contact times tend to be too long to allow examination of dissolution limitations at less than 1 day – if there is a process-development interest in distinguishing between a process that takes an hour and a process that takes a day.
2. The type of slurry agitation applied in the laboratory setting is not quantified in terms of the particle slip velocity, or turbulence, that it induces. It is therefore impossible to generalize the results to processes where different slip velocities or turbulence levels exist, and these are the properties that control the mass-transport limits on dissolution rates.
3. The tests did not assess whether equilibrium had been reached at the end of each step before adding more solvent.
4. Most of the dissolution in these tests has occurred under conditions where the dissolution of highly soluble sodium nitrate, or of moderately soluble later-dissolving salts such as sodium carbonate, dominates dissolution behavior. If there is a desire to dissolve (for example) waste heels where fluoride salts predominate, dissolution tests on wastes or simulants of that kind are needed.

6.2 Other Observations on Hanford Waste

There have been two observations of slow villiaumite (NaF) dissolution that were not made in sequential waste dissolution tests. One involved water leaching of a high-fluoride sample from AW-105; the other, reconstitution of an AW-103 sample after a boil-down test.

The AW-105 sample consisted of solids that were subjected to washing with inhibited water (Huber 2013). The solids consisted of 90% villiaumite, with no evidence that any substantial fraction of the fluoride was present in a zirconium oxyfluoride form. Sodium was present predominantly as villiaumite or sodium zirconium oxide; the latter was thought not to have been dissolved by leaching.

There were three leaches, each using about 1:1 water:waste by mass. Although the total contact time over the three washes was 912 h, agitation during the contact was not continuous: “jars were shaken at least twice daily for several minutes.” At the end of leaching, about half the fluoride had been leached and villiaumite crystals were still present in the waste. Optical microscopy images showed villiaumite particles with sizes of 20 to 30 μm both before and after leaching. Complete size distributions were not measured, so the change of the average particle size is unknown. However, the original crystals were observed to be smooth-sided with nearly perfect structure, while the leached crystals were rough and deeply fissured.

These observations suggest that, at least under primarily stagnant conditions, villiaumite leaching may not involve the entire waste surface equally. Some parts of the surface were more susceptible to dissolution than others, perhaps simply because they were not covered up by other particles. Since villiaumite was the dominant soluble solid containing sodium or fluoride, common-ion effects would have been limited.

Callaway et al. (2020) described another case of slow dissolution of villiaumite (NaF). A composite of clear liquid grab samples from AW-103 was boiled down to about 48% of its original volume and then reconstituted to its initial volume by several steps of dilution with water. The composite was stirred during boil-down and re-dilution using a magnetic stir bar. Despite the return to the original volume and species concentrations, the reconstituted samples were cloudy, containing a small volume of clear, fine-grained solids. After stirring was stopped, the solids settled ~ 7.5 cm in 8 to 10 h and did not re-dissolve perceptibly in that time. The wet bulk solids amounted to about 1 wt% of the reconstituted material, and chemical analysis results indicated that sparingly soluble fluoride solids, probably villiaumite, could be a major component of the remaining solids. Since villiaumite was the first solid to precipitate during boil-down, its dissolution after re-dilution was probably at near-saturation conditions, one factor that would lead to a low re-dissolution rate.

7.0 Dissolution Rate

The rate of dissolution of a solid is controlled by both the surface reaction rate – the rate at which ions or complexes are detached from the solid surface into the liquid at the surface – and the rate of mass transfer from the surface liquid to the bulk liquid. When the mass transfer rate is rapid compared to the reaction rate, the surface reaction rate is the limiting rate and the liquid at the surface can be assumed to have the same concentration as the bulk liquid and to be below the saturation concentration. When the mass transfer rate is slow compared to the reaction rate, mass transfer is the limiting rate and the liquid at the surface can be assumed to have approximately a saturation concentration.

In circumstances where the surface reaction is a simple first-order reaction in the solute concentration, the overall dissolution rate, k , can be calculated as

$$k = \frac{1}{\frac{1}{k_c} + \frac{1}{k_{SL}}} \quad (4)$$

where k_c is the surface reaction rate constant (m/s) and k_{SL} is the mass transfer rate constant (m/s). This equation is used by Alkattan et al. (1997) for sodium chloride in water under the condition that sodium and chloride concentrations in the liquid are close to equal – i.e., dissolution occurs without significant concentrations of common ions. This is a significant limitation for many Hanford dissolution applications, because Hanford wastes typically contain substantial sodium (beyond that derived from fluoride salt dissolution) and often contain other sources of sulfate and phosphate as well. The absence of a reaction/transport expression for more general conditions is a significant gap, which is discussed further in a later section.

Both mass-transfer rate and surface reaction rate are discussed in the remainder of this section.

7.1 Single-Salt Dissolution Rate – Limited by Mass Transfer

The mass-transport theory discussed in this report considers only mass transfer from particles to liquid. Mass transfer from an effectively flat, consolidated surface into liquid being sluiced over the waste surface is not considered, nor is mass transfer in liquid percolating through waste pores. If the processes intended for fluoride dissolution include sluicing or percolation, the lack of development of suitable mass-transfer models is a gap.

Mass transfer from, or to, a particle in liquid is provided by both molecular diffusion (which sets the lower bound) and eddy diffusion. The mass-transfer coefficient, k_{SL} , depends on solid density (or density difference from the liquid), particle shape and size, solids concentration, extent of suspension of particles, liquid viscosity, diffusivity of solutes, turbulence in the liquid, and dimensions of the equipment (Bong 2013). Many correlations for k_{SL} have been developed. A number of correlations for impeller-agitated vessels are listed by Bong (2013), who regards none of them as universal and gives a general form for such correlations as

$$Sh = 2 + BRe^m Sc^n \quad (5)$$

where Sh is the particle Sherwood number (the ratio of k_{SL} to the molecular diffusion rate), B is a correlation constant, Re is a particle Reynolds number whose definition varies from one model of solid/liquid hydrodynamic interaction to another, Sc is the Schmidt number for the solute/liquid

combination, and the exponents m and n may be derived either from correlation or theory. The first term of Eq. (5), the dimensionless value of 2, represents molecular diffusion, the second eddy diffusion.

For an impeller-agitated tank, the Reynolds number may be based on one of three types of models: (1) the impeller-tip velocity, (2) the slip velocity between particle and liquid (the minimum value being the terminal settling velocity), or (3) the rate of turbulent energy dissipation, based on Kolmogoroff's theory of turbulence. For the purposes of this report, a correlation based on the slip velocity will be used, since neither the impeller nor the power input is defined for Hanford processes where dissolution will occur. It is understood that the slip velocity in Hanford dissolution processes – even in laboratory dissolution studies in mixed beakers – will be higher than the particle terminal velocity because of local fluid acceleration and the difference between the actual drag coefficient and that under terminal settling conditions. The slip velocity cannot be defined at this time, but the use of a lower bound (the terminal settling velocity) will help provide an understanding of the functionality of k_{SL} .

The mass-transfer coefficient correlation selected for this report was based on solids concentrations between 5 and 40 vol%. The definitions of the dimensionless Reynolds and Schmidt numbers have been substituted into the equation as given below:

$$\frac{k_{SL}d_p}{D_A} = 2 + 0.95 \left(\frac{u_s d_p \rho_L}{\mu_L} \right)^{0.5} \left(\frac{\mu_L}{\rho_L D_A} \right)^{0.33} \quad (6)$$

This correlation is similar in form to others given by Bong (2013) for the slip-velocity model, but the particular exponents and coefficients are taken from the model that Bong (2013) attributes to Cline. No definition is given for the range of Reynolds number and Schmidt number for which the correlation holds. Practically speaking, the fluid velocities would have been intended to fully suspend the solids, and flow conditions are likely to have been turbulent.

The parameters on which k_{SL} depends are the particle diameter d_p , solute diffusivity D_A , slip velocity u_s , liquid viscosity μ_L , and liquid density ρ_L . Solving for k_{SL} gives

$$k_{SL} = 2 \frac{D_A}{d_p} + 0.95 \frac{D_A^{2/3} \rho_L^{1/6}}{d_p^{1/2} \mu_L^{1/6}} u_s^{0.5} \quad (7)$$

The terminal velocity used as an estimate of slip velocity was taken from Wells et al. (2011) and Camenen (2007). The closed-form equation for the terminal velocity of a settling sphere, u_t , is

$$u_t = \frac{\mu_L}{\rho_L d_p} \left[\sqrt{15 + \sqrt{\frac{(\rho_p - \rho_L) \rho_L g d_p^3}{0.3 \mu_L^2}}} - \sqrt{15} \right]^2 \quad (8)$$

where ρ_p is the particle density and g is the acceleration of gravity. In the above equation, it is assumed that the particle concentration is low enough to preclude hindrance of settling. Camenen (2007) also gives settling velocity parameters for other shapes of particles, but it would not be consistent to use them with a mass-transfer correlation based on spherical particles.

For any given type of mixing, slip velocities will vary with location in the process vessel. As an example, Fishwick et al. (2003) carried out tests in a turbine-mixed vessel where the impeller diameter, 0.033 m,

was one-third the diameter of the vessel, the impeller speed was 800 rpm (an impeller tip speed of 1.4 m/s), and the liquid was water. For spherical particles of approximately 250 μm diameter with a density of 3009 kg/m^3 , slip velocities (measured by positron emission particle tracking) were less than 0.2 m/s in 50% of the suspension volume, between 0.2 and 0.5 m/s in 40% of the volume, and between 0.5 and 1.0 m/s in the remaining 10%. These velocity data were effectively instantaneous, since it was typical for a tracer particle position to be measured about 250 times per second.

As would be expected, slip velocity was higher than terminal settling velocity in this actively mixed system. These particles would be expected to have a terminal settling velocity of 0.028 m/s, based on Eq. (8). For this example, in a small percentage of the volume, the slip velocity was half or more of the driving velocity: that is, the impeller tip velocity. The terminal velocities are used in the current report to calculate lower bounds on slip velocities in actively mixed systems.

To calculate mass-transfer-controlled dissolution rates, start with the following assumptions:

- A single salt, present as a monodisperse spherical particle, is dissolving into water, or into a solution of that same salt, under mass-transfer limited conditions.
- Outside the mass-transfer “film,” the bulk of the liquid is well-mixed.
- The acid/base dissociation behavior of the salt anion is negligible.
- The liquid volume V_L changes negligibly as the result of addition of solute during dissolution.
- The equilibrium and actual salt concentrations are low enough that the activity coefficients are near unity, allowing concentration to be used rather than activities.

The dissolution rate mass balance is

$$\frac{dN}{dt} = -k_{SL}A_p(C_S - C_{Sdiss} - C_{S0}) = -k_{SL}A_p\left(C_S - \frac{N_0 - N}{V_L} - C_{S0}\right) \quad (9)$$

where N is the moles of solid at time t , N_0 is the initial moles of solid, A_p is the effective particle area, k_{SL} is the mass-transfer coefficient, C_S is the dissolved concentration of the salt at saturation, C_{Sdiss} is the concentration produced solely by dissolution of the particle, and C_{S0} is the dissolved salt concentration (if any) that was present before the particle began to dissolve. The rate depends on the mass-transfer coefficient, the particle surface area, and the driving force, which is the concentration difference between the liquid at the particle surface (assumed to be at saturation concentration C_S) and the concentration in the bulk liquid (the sum of the initial concentration and the increment produced by dissolution).

If we express the moles of solid in terms of particle molar density, ρ_M , and put the particle volume and area in terms of particle diameter, the result is

$$\frac{dd_p}{dt} = -2k_{SL}\left(\frac{1}{d_{p0}^3} \frac{V_{p0}}{V_L} d_p^3 - \left(\frac{C_S - C_{S0}}{\rho_M} - \frac{V_{p0}}{V_L}\right)\right) \quad (10)$$

Here the ratio V_{p0}/V_L is the initial ratio of solid/liquid volume. This ordinary differential equation (ODE) is separable, though the dependence of k_{SL} on particle diameter makes it solvable only by numerical integration.

Because the equation is separable, it can be integrated to find the dissolution time in terms of the initial diameter and a final diameter:

$$t = - \int_{d_{p0}}^{d_p} \frac{dd_p}{2k_{SL} \left[\frac{1}{d_{p0}^3} \frac{V_{p0}}{V_L} d_p^3 + \left(\frac{C_S - C_{S0}}{\rho_M} - \frac{V_{p0}}{V_L} \right) \right]} \quad (11)$$

The inputs for the integrated ODE model are given in Table 1. Note that one of the two solids modeled is “pseudo-natrophosphate”; this is defined as a hypothetical single salt that has the properties of natrophosphate [Na₇F(PO₄)₂·19H₂O], which is a double salt and outside the strict range of applicability of the model. “Pseudo-natrophosphate” is used to demonstrate the effect of different solid properties and particle sizes. It is not clear that the results would describe actual natrophosphate, although they should be meaningful in terms of order-of-magnitude estimates.

Many of these input values are found either in Wells et al. (2011) or in standard references. Others are chosen to reflect a given scenario. Three different particle sizes were modeled for pseudo-natrophosphate, and one for villiaumite, all within ranges described in Section 4.0. The initial liquid is assumed to be pure water, and the initial particle/water volume ratio is set at a minimum-water value that would give saturation concentration at exactly 100% dissolution. The value is calculated as

$$V_{p0}/V_L = (C_S - C_{S0})/\rho_M \quad (12)$$

This concentration scenario is a compromise between dissolution at optimal conditions with an excess of pure water and dissolution at conditions where the liquid is initially partway to saturation.

The saturation concentration inputs were chosen to be consistent with 25 °C data presented in Section 5.1 and Section 5.3. A value of 0.98 M was used for villiaumite (NaF). The value of 0.11 M, for pseudo-natrophosphate, was taken from measurements made without excess fluoride or phosphate in solution: that is, near the stoichiometric ratio for the two ions. This was appropriate for the assumed stoichiometric dissolution of natrophosphate [Na₇F(PO₄)₂·19H₂O] in pure water.

The diffusion coefficients, assumed to be 1 × 10⁻⁹ m²/s, are approximate within a factor of 2 in either direction. Because the solute is present in ionic form and ions must diffuse in manner that maintains charge balance in the liquid (Boudreau et al. 2004), each ion’s diffusion coefficient is to some extent dependent on the concentrations and charges of other ions that are diffusing. A cation that would normally diffuse rapidly might be slowed to maintain charge balance with anions that move slowly because of, for example, greater molecular weight.

Poisson and Papaud (1983) provide estimates of diffusion coefficients of seawater ions in solutions of various concentrations. Those values ranged from about 7 × 10⁻¹⁰ m²/s to 2 × 10⁻⁹ m²/s at 25 °C, depending on the ion and the salinity gradient being tested. Alkattan et al. (1997) found a diffusion coefficient of 2.2 ± 0.4 × 10⁻⁹ m²/s for sodium chloride near saturated concentration at 25 °C. Taking the range of data into account, an approximate diffusion coefficient of 1 × 10⁻⁹ m²/s is used in modeling both pseudo-natrophosphate and villiaumite (NaF). It is understood that the references used are not exhaustive, that the mass-transfer coefficient depends strongly on the diffusion coefficient, and that dissolution modeling would benefit from more specific information.

The integrated ODE, together with Eqs. (7) and (8), was used to estimate terminal velocities, mass-transfer coefficients, and the time required to dissolve 99 vol% of the solid. The modeling results are presented in Table 2, with the dissolution time given to one significant figure.

Table 1. Inputs for Order-of-Magnitude Modeling of Mass-Transport-Controlled Dissolution

Pseudo-natrophosphate [Na ₇ F(PO ₄) ₂ ·19H ₂ O]	Villiaumite (NaF)	Input
1750	2780	ρ_p , particle mass density (kg/m ³)
997		ρ_L , liquid density, ambient water (kg/m ³)
8.9×10^{-4}		μ_L , viscosity; ambient water (Pa s)
1.0×10^{-9}		D_A , diffusion coefficient for solute (m ² /s)
712.17	41.99	molecular weight
2457	66206	ρ_M , particle molar density (mol/m ³)
110	980	C_S , liquid saturation concentration (mol dissolved/m ³)
0		C_{S0} , liquid concentration at t=0 (mol dissolved/m ³)
0.0448	0.0148	V_{p0}/V_L , particle/liquid volume ratio at t=0
100, 2000, 6000	100	particle diameter at t=0 (μm)

Table 2. Predictions from Order-of-Magnitude Modeling of Mass-Transport-Controlled Dissolution

	Initial Unhindered Terminal Velocity u_t (m/s)	Slip Velocity $u_s =$ Terminal Velocity		Slip Velocity $u_s =$ Zero (stagnation)	
		Mass- Transfer Coeff. k_{SL} (m/s)	Time to Reach 99% Dissolution	Mass- Transfer Coeff. k_{SL} (m/s)	Time to Reach 99% Dissolution
Villiaumite (NaF), 100 μm	8.6×10^{-3}	1.1×10^{-4}	5 min	2.0×10^{-5}	10 min
Pseudo-natrophosphate [Na ₇ F(PO ₄) ₂ ·19H ₂ O], 100 μm	3.9×10^{-3}	8.1×10^{-5}	2 min	2.0×10^{-5}	4 min
Pseudo-natrophosphate [Na ₇ F(PO ₄) ₂ ·19H ₂ O], 2 mm	1.6×10^{-1}	8.7×10^{-5}	0.7 hr	1.0×10^{-6}	1 day
Pseudo-natrophosphate [Na ₇ F(PO ₄) ₂ ·19H ₂ O], 6 mm	3.3×10^{-1}	7.2×10^{-5}	2 hr	3.3×10^{-7}	9 days

Despite the substantially lower solubility of natrophosphate, a villiaumite sphere is predicted to dissolve half to one-third as fast as a pseudo-natrophosphate sphere of the same diameter. This outcome is not immediately intuitive, but is consistent with the form that Eq. (10) takes for the selected initial ratio of V_{p0}/V_L , equal to $(C_S - C_{S0})/\rho_M$:

$$\frac{dd_p}{dt} = -2k_{SL} \left(\frac{1}{d_{p0}^3} \frac{C_S - C_{S0}}{\rho_M} d_p^3 \right) \quad (13)$$

The predictions for different sizes of pseudo-natrophosphate [Na₇F(PO₄)₂·19H₂O] spheres show that the initial mass-transfer coefficient at a slip velocity equal to the terminal velocity does not vary strongly with initial particle diameter. The increase in slip velocity and mass-transfer coefficient with increasing diameter offsets the decrease in mass-transfer coefficient that is directly produced by increased diameter.

This case may be a reasonable match to laboratory dissolution of small samples where agitation is produced by end-over-end tumbling – for example, the stepwise waste dissolution tests presented in Section 6.0.

On the other hand, in stagnant conditions the mass-transfer coefficient is inversely proportional to diameter and larger particles show a substantial decrease in dissolution rate. This behavior would be mechanistically similar to that in tests where dilution water was added to waste and mixing was infrequent over the contact period – for example, the AW-105 water washes discussed in Section 6.2. However, the dissolution rate in such tests would have been even lower than shown in Table 2 because the particles in the tests were not suspended in liquid. For most of the contact time, only the particles at the top would have been exposed to supernatant liquid, over part of their surfaces, and other particles would have been exposed only to pore liquid. The dissolution rate would be increased by using more solvent per volume solid and decreased by the presence of a non-zero concentration of the salt in the solvent – as would happen if supernatant from another tank was used as solvent. The effect of these scenario inputs has not been explored here, but the model could be used to provide an approximate evaluation.

The concerns with using the mass-transport model described in this section are as follows:

- The diffusion coefficient could be a factor of 2 higher or lower than the modeled value, depending on the ionic composition in the liquid. Based on Eq. (7), a factor of 2 difference in diffusion coefficient gives a factor of 2 difference in rate at stagnant conditions, or a factor of $2^{2/3}$ (~1.6) difference in rate at high slip velocity. It is likely that the diffusion coefficient for villiaumite is higher than the modeled 1×10^{-9} m²/s, at least when villiaumite is dissolved in pure water, based on the value measured for the analogous and higher-molecular-weight salt sodium chloride by Alkattan et al. (1997). The diffusion coefficient of pseudo-natrophosphate would probably be lower than that of villiaumite because of the high molecular weight of the phosphate ion. However, the value of the diffusion coefficient is not known in liquids of higher ionic concentration than that produced by dissolution of the fluoride solids. Nor is it known in the presence of fluxes of other ions whose gradients would impose charge-balance constraints on the flux of fluoride salt ions.
- Waste particles are polydisperse, so the relatively rapid dissolution of small particles of a solid would delay the dissolution of the larger particles. Given the difference in time scales between the different particle sizes modeled here, it should be possible to estimate the effect of polydispersity by modeling in steps. First, model the fraction of the solid that has the smallest particles. Take the resulting dissolved concentration and the solid/liquid ratio for the next larger size, use them as inputs to modeling the next larger size, and so on. Then, add the times for each particle size together to get the overall time.
- The common-ion effect of other salts has not been accounted for and cannot be, because of the assumption that there is only one salt present. The presence of, for example, 1 M sodium nitrate in the solvent would affect the equilibrium concentration of dissolved villiaumite (NaF). It might also affect diffusion through changing the fluoride, sulfate, or phosphate diffusion coefficient. The model is suitable only for water solvent or very dilute supernatants or solutions (like inhibited water). Some thought needs to be given to whether inputs to this model could be adjusted to account for the equilibrium effect of common ions.
- Slip velocities for Hanford processes are not known and would vary with location in the vessel. The slip velocity has a substantial effect on mass-transfer.

7.2 Single-Salt Dissolution Rate – Limited by Surface Reaction

Per Eq. (4), dissolution rate is controlled by both a mass-transfer rate constant and a surface reaction rate constant. The combination of the two constants into an overall rate constant cannot be assessed, even for the simple case of a single salt dissolving in pure water, without experimental data.

A literature search did not locate any articles or reports describing the dissolution rate of villiaumite. This section therefore discusses reaction rate constants measured under different conditions for sodium chloride in water by Alkattan et al. (1997), as a way of comparing reaction rate and mass-transfer rate constants. On the assumption that sodium chloride (NaCl) and villiaumite (NaF) behave similarly, the surface reaction rates may provide insight into the mechanism controlling villiaumite dissolution. This assumption is meant purely for illustrative purposes because the solubilities of NaCl and NaF are so different as to imply a possible difference in kinetic behavior as well. In addition, HF is a weak acid and HCl a strong acid; therefore, H⁺ ion is more likely to be involved in the surface reaction mechanism for NaF than for NaCl.

The tests carried out by Alkattan et al. (1997) used disks of compressed sodium chloride set in resin so that one face of the disk was free. The disk was rotated for a chosen amount of time below the solution surface at several different speeds or at 300 rpm, depending on the test. Tests of the temperature effect were made at a range of speeds at near-saturation concentrations. A linear fit of the measurements of inverse rate to inverse square root of the rotation speed allowed the surface reaction and mass-transfer contributions to the dissolution rate to be separated so that surface reaction coefficients and diffusion coefficients could be calculated. Other tests were made at one speed, 300 rpm, and one temperature, 25 °C. The surface reaction rate was calculated by correcting for the mass-transfer contribution to dissolution rate, based on the diffusion coefficient that had been determined at 25 °C and on a standard correlation for mass-transfer coefficient from the rotating disk.

Table 3 shows the experimental surface reaction rate constants that were obtained under different conditions of temperature and trace metal concentration. The experimental contact time at a given speed was an additional variable, and the time for tests at ~300 rpm is therefore included in the table. The NaCl diffusion coefficients that were measured at the three temperatures were 2.2×10^{-9} , 3.55×10^{-9} , and 6.00×10^{-9} m²/s at 25 °C, 50 °C, and 80 °C, respectively.

Alkattan et al. (1997) assessed the effect of trace metal chlorides on dissolution rate (not reaction rate constant) as inhibiting the dissolution of sodium chloride in this order of effectiveness: CdCl₂ > PbCl₂ > CrCl₃ > CoCl₂ > ZnCl₂ = FeCl₃. This order is also approximately followed by the reaction rate constants shown in Table 3, although the use of more than one contact time in testing adds some ambiguity to the interpretation. The test results showed that, as the concentration of cadmium and lead increased slightly from zero, inhibition of dissolution rate increased rapidly and remained about constant for all higher metal concentrations. For the other inhibiting metals, the effect was much more gradual as concentration increased.

The authors rejected the reaction-controlling mechanism of cadmium/sodium exchange at the surface. They theorized that a trace metal and a chloride ion attached simultaneously to the sodium chloride surface, obstructing dissolution sites on the surface, and that the strength of inhibition of a trace metal therefore increased with its ability to form strong metal chloride complexes. They proposed Hg⁺² as another possible strong inhibitor. For villiaumite (NaF), the strength of dissolution inhibition would depend on the strength of metal-fluoride complexation.

Table 3. Measured Surface Reaction Constants or Dissolution Rates for Sodium Chloride in Water (Alkattan et al. 1997)

Test Condition	Surface Reaction Rate Constant (m/s)
Temperature tests	
Water, 25 °C, saturation 94% 10 min @ 300 rpm	5.0×10^{-4}
Water, 50 °C, saturation 93% 10 min @ 300 rpm	2.1×10^{-4}
Water, 80 °C, saturation 90% 15 min @ 340 rpm	1.2×10^{-4}
Trace metal tests	
0.01 M ZnCl ₂ , 25 °C, sat. 94% 20 min @ 300 rpm	2.0×10^{-4}
25 min @ 300 rpm	4.0×10^{-4}
0.01 M CoCl ₂ , 25 °C, sat. 94% 20 min @ 300 rpm	1.6×10^{-4}
0.01 M CrCl ₃ , 25 °C, sat. 94%, 20 min @ 300 rpm	1.7×10^{-4}
0.01 M CdCl ₂ , 25 °C, sat. 94% 10 min @ 300 rpm	7.7×10^{-6}
20 min @ 300 rpm	7.4×10^{-6}
0.0099 M PbCl ₂ , 25 °C, sat. 94% 10 min @ 300 rpm	1.9×10^{-5}
0.01 M FeCl ₃ , 25 °C, sat. 94% 10 min @ 300 rpm	2.3×10^{-4}

Accepting for illustrative purposes that the sodium chloride surface reaction rates in Table 3 might be roughly applicable to villiaumite (NaF) dissolving in water, they can be compared to the mass-transfer coefficients for a 100- μ m villiaumite particle in Table 2, 1.1×10^{-4} m/s for terminal velocity and 2.0×10^{-5} for stagnant conditions. At terminal velocity and 25 °C, for metals other than cadmium and lead the surface reaction rate coefficients are higher than the mass-transfer coefficient and therefore are not dissolution-rate-limiting. From Eq. (4), the overall rate coefficient would be somewhat lower than the mass-transfer coefficient at terminal velocity and about the same as the mass-transfer coefficient at stagnation. For cadmium, the surface reaction rate coefficients are considerably less than the mass-transfer coefficient whether at stagnation or terminal velocity; surface rate reaction is controlling. The effect of lead is similar for a 100- μ m particle at terminal velocity. Larger particles under stagnant conditions would have mass-transfer-limited dissolution.

Note that in sodium chloride dissolution processes with agitation, the slip velocity could easily be a factor of 10 higher than terminal velocity. Under those conditions, the rate would be controlled by the surface reaction rate constant for all of these trace metals. The same could be true for villiaumite dissolution. Figure 5 illustrates the dissolution times for two different sizes of villiaumite particles – 100 μ m and 6 mm – subjected to a range of different slip velocities, based on modeling with the same parameters given in Table 1.¹⁵ The y-axis (1×10^{-6} m/s) approximates stagnation conditions. Between stagnation and 1 m/s slip velocity, the dissolution time – if controlled by mass-transfer alone – decreases by a factor of about 100 for the large particle and about 10 for the small particle. The effect of slow surface-reaction rate can be seen by noting that, per Eq. (4), dissolution would be equally controlled by surface-reaction

¹⁵ 6-mm villiaumite particles have not been observed in waste, but are used to illustrate the effect of particle diameter.

rate and mass-transfer rate when the two rates are equal. A surface-reaction rate of about 1×10^{-5} m/s would give an overall dissolution rate that was half the mass-transfer rate at the slip velocity where the mass-transfer coefficient was equal to 1×10^{-5} m/s. The slip velocity at 1×10^{-5} m/s mass transfer coefficient is indicated by the arrows in Figure 5. For the assumed surface-reaction rate, the dissolution time would level off at higher velocities, meaning that the large particle would require at least 1×10^5 seconds (~30 h) to dissolve, and the small particle would have the same dissolution time as at stagnation, no matter how high the agitation employed.

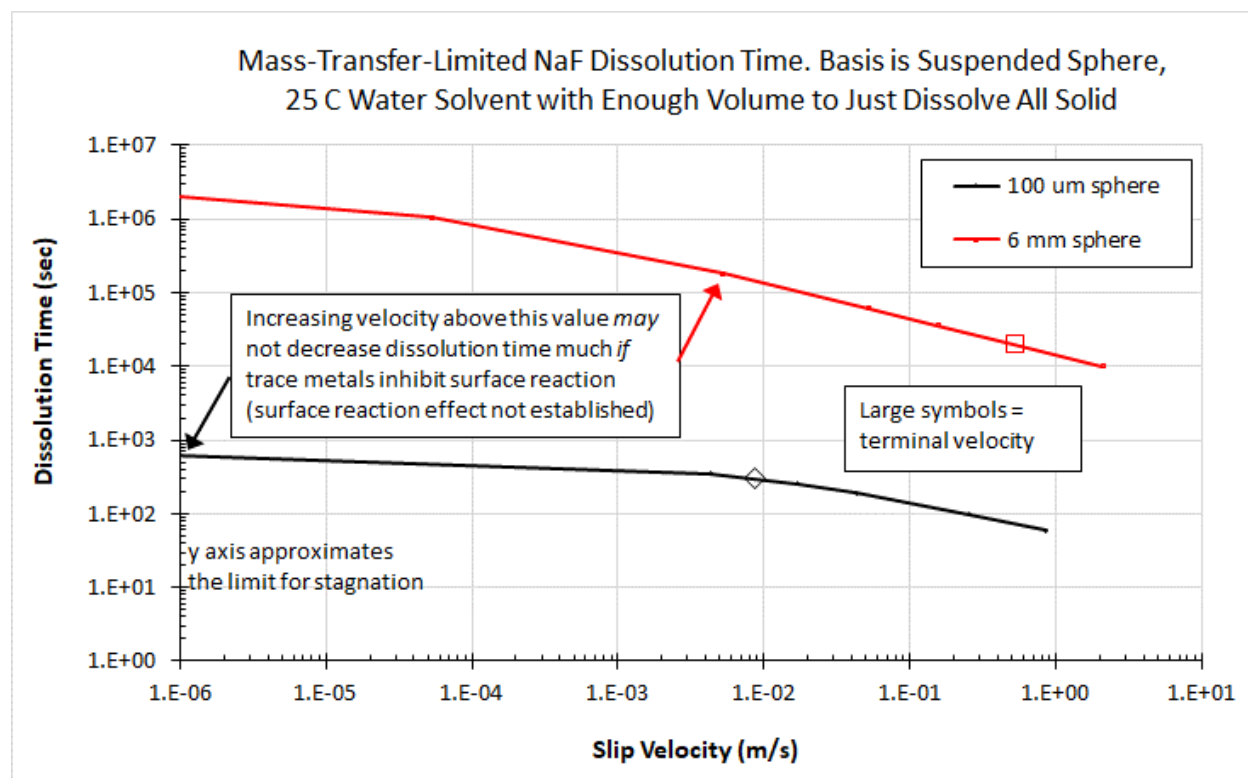


Figure 5. Mass-Transfer Dissolution Time as a Function of Particle Size and Slip Velocity

Alkattan et al. (1997) also studied the dependence of sodium chloride surface reaction rate on saturation fraction, for pure water at 270 rpm and 0.01 M CdCl₂ at 300 rpm, both at 25 °C. Dissolution rate was a linear function of the fractional saturation for pure water as the solvent. The presence of trace cadmium decreased the surface reaction rate below linearity – presenting a concave-upward curve – with the percentage decrease in rate becoming more significant as saturation fraction increased. Thus, the strong inhibiting effect of cadmium that was found at 94% of saturation (Table 3) was less important for sodium chloride dissolution at low saturation.

The information presented in this section suggests that in a complex dissolved-waste environment, where many trace metals are present, it is possible that surface reaction rate will control dissolution of villiamite. If that is the case, increased agitation would not increase the dissolution rate and would not be an efficient use of energy. However, the Alkattan et al. (1997) data did not address the presence of substantial amounts of other sodium salts in solution; the effect of these anions and cations is unknown.

7.3 Double-Salt Dissolution Rates – Theory

A literature search did not locate any articles or reports about the dissolution rate of the double salts natrophosphate [$\text{Na}_7\text{F}(\text{PO}_4)_2 \cdot 19\text{H}_2\text{O}$] and kogarkoite (Na_3FSO_4). However, Dorozhkin (2012) reviewed mechanisms that have been suggested, and observations that have been made, for the dissolution of calcium hydroxyapatite [“HA”, formula $\text{Ca}_{10}(\text{PO}_4)_6(\text{OH})_2$] and fluorapatite [“FA”, formula $\text{Ca}_{10}(\text{PO}_4)_6\text{F}_2$] in acids. These are double salts, one of them containing fluoride, and are worth considering conceptually because of that partial similarity to the fluoride double salts in Hanford waste.

The mechanisms listed by Dorozhkin (2012) as being pertinent to surface reaction rate are not described here in apatite-specific detail, but in more general terms. The hypothesized mechanisms include the following:

- (a) A molecular detachment mechanism. Mononuclear detachment starts from a single point and spreads over the surface, whereas polynuclear detachment simultaneously spreads from multiple centers, possibly at steps in the crystal surface. For HA, different types of detachment have been observed in different pH ranges.
- (b) Self-inhibition. In some pH ranges, re-adsorption of calcium ion is believed to form a calcium-rich layer, causing reduction in dissolution rate. However, this layer has been inferred indirectly, not confirmed by direct measurement of surface composition.
- (c) Incongruent dissolution. Some measurements of liquid composition have shown that, in acidic dissolution of FA, fluoride ions have been found to enter solution more rapidly than ions of calcium, and calcium ions more rapidly than phosphate ions. However, other tests have shown non-stoichiometric dissolution with the opposite tendency, or even stoichiometric (congruent) dissolution kinetics. The differences may have arisen from different pH levels or from the presence or absence of co-anions (such as sulfate, acetate, or chloride). The indications from liquid composition measurement are that a calcium-depleted layer forms, in contradiction to the self-inhibition model in (b).
- (d) Dissolution resulting from four successive chemical reactions, rather than detachment of single-molecule units each containing 18 ions.
- (e) Etch pit formation. Structural defects in the apatite crystals induce dissolution, which continues as steps spread out over the surface.
- (f) Ion exchange. For dissolution of apatite in acid, hydrogen ions and acid anions (such as citrate) adsorb onto the apatite surface in exchange for the removal of calcium and phosphate ions. This mechanism appeared in relatively low concentrations of citric acid/citrate, but not at higher concentrations.
- (g) Catalysis by hydrogen ion. The protonation of the apatite surface converts phosphate ions into hydrogen phosphate ions, hypothetically increasing release rate. For FA, protonation may also convert fluoride ion to HF. Only indirect data were available to support the catalytic effect.

The general conclusion to be drawn from the observations, and from the models hypothesized to explain them, is that surface reaction rates of double salts can be controlled by multiple mechanisms, each potentially dominating in a different set of conditions. Variables such as pH, common ions, and other cations and anions may all play a part. Experimental data for the dissolution regimes of interest are essential, since no *a priori* decision can be made about the controlling mechanism.

It is also worth noting that Dorozhkin (2012) states that dissolution of apatite sometimes passes through an incongruent (non-stoichiometric) stage. This is pertinent to natrophosphate [$\text{Na}_7\text{F}(\text{PO}_4)_2 \cdot 19\text{H}_2\text{O}$]

dissolution. A Hanford study of natrophosphate precipitation from simulants containing sodium, aluminate, and hydroxide ions together with stoichiometric 2:1 proportions of phosphate of fluoride showed transient incongruent precipitation in some of the tests (Reynolds and Herting 2016). The earliest precipitate was $\text{Na}_3\text{PO}_4 \cdot 0.25\text{NaOH} \cdot 12\text{H}_2\text{O}$. After a period of days to weeks, the solid recrystallized to natrophosphate. Considering this observation during precipitation, and the observations for FA, it is an open question whether dissolution of the double salts natrophosphate and kogarkoite would proceed by first releasing fluoride and then the other anion, or vice versa. The manner in which the incongruent behavior might depend on the dissolution conditions – fluoride or phosphate in excess of stoichiometric, or presence of other ions – is also not known. The behavior of kogarkoite (Na_3FSO_4) in this respect is also not known.

There is also some question about whether dissolution might end before reaching full equilibrium. Dorozhkin (2012) states that apatite dissolution has sometimes been observed to end before reaching the expected complete dissolution, suggesting either that a kinetically metastable state was reached or that the expected solubility was an overestimate. Crundwell (2017) also refers to a “partial equilibrium” that produces a premature end to dissolution for copper sulfide. The author explains this in terms of the anion and cation of the mineral being released from the surface at different rates, not only producing a surface charge but making it possible for one ion to reach its equilibrium before the other does.

Crundwell (2017) discusses examples of surface charge on minerals and its relationship to dissolution, and proposes that the interaction between surface charge and rate of ion release is yet another mechanism potentially controlling surface reaction rate. The article provides a substantial analysis of the way in which surface charge (i.e., surface potential) might define the function that describes the dependence of the dissolution rates on saturation fraction. This function is not necessarily linear. Crundwell (2017) presents the example of albite, for which the function was sigmoidal. Dissolution rates were high over the low end of the saturation range, then decreased steeply over a short range of saturation, then held at slow dissolution rate not just near saturation but over a range of high saturation. If the fluoride double salts show this behavior, the result would be that dissolution could be extremely slow after only partial removal of solid.

8.0 Observations, Conclusions, Gaps, and Recommendations

The following are the gaps in the information about fluoride salt dissolution, that is, the information that is complete enough to allow conclusions to be drawn, and approaches that could be taken to improve dissolution rate estimates.

From Section 3:

Gap: The specifics of the dissolution process at Hanford are not defined well enough to provide a focused direction for further work. Process parameters to be defined are the solvent, the solvent temperature, the extent to which fluoride salt particles will be suspended and agitated in the liquid, and the extent to which more-soluble salts such as nitrate will still be present. The relevancy of suspended-particle dissolution rate predictions cannot be assessed without this information.

From Section 4:

Conclusion: It is sufficiently well established that the fluoride compounds of concern in Hanford dissolution are villiaumite (NaF), natrophosphate [$\text{Na}_7\text{F}(\text{PO}_4)_2 \cdot 19\text{H}_2\text{O}$], and kogarkoite (Na_3FSO_4), and that cryolite, fluorozirconates, and fluorosilicates, if present, contain much less of the fluoride loading in the waste. Large aggregates or crystals of the double salts natrophosphate and kogarkoite – 5 mm and up – have been observed both in the C-108 waste heel and in AP-107. Natrophosphate has also been found in a C-108 hardpan layer in conjunction with trona.

From Section 5:

Observation: When water is the solvent, phosphate or fluoride acid/base behavior may increase the effective solubility of natrophosphate [$\text{Na}_7\text{F}(\text{PO}_4)_2 \cdot 19\text{H}_2\text{O}$] and villiaumite (NaF). In addition, the presence of waste-derived carbonate as a buffer might hold pH at a level where the solubility of natrophosphate is increased. The use of river water or inhibited water (at 0.01 M NaOH and 0.011 M NaNO_2) [Uytioco 2015]) for dissolution might allow for this lower-pH enhanced solubility, but more-concentrated caustic would not (aside from reducing dissolution by the common-ion effect of sodium).

The solubility of natrophosphate can be a factor of 10 higher at 50 °C than at 25 °C, whether other anions are present in solution or not. For villiaumite, when other anions are present there is no clear effect of temperature on solubility; when other anions are absent, a small increase in solubility with temperature is observed. For kogarkoite (Na_3FSO_4), there is no clear effect of temperature on solubility, but the data for kogarkoite are too sparse to allow a firm conclusion. One implication is that increasing the solvent temperature would provide an advantage in dissolving natrophosphate versus the other two fluoride salts.

Gap/Recommendation: If kogarkoite is a large part of the fluoride inventory in Hanford waste, the effect of temperature on its solubility needs to be studied both for kogarkoite in water and for kogarkoite in simulant solutions representing plausible dissolution conditions. The database for thermodynamic models used in process evaluations should be updated with or tested against the new information.

From Section 6:

Gap: Past dissolution tests on Hanford waste samples have not provided much information about dissolution rates of fluoride salts (or other salts). In most cases, the contact time was about a day, so there is no information on rate behavior over shorter times. In shorter tests, contact time was not well defined.

In percolation tests, the water addition time was known but there was no quantitative estimate of the contact time. In mixing tests, centrifugation time contributed to contact time to an extent that could be significant.

Gap: The contact velocity (slip velocity) between the particles and the liquid was not estimated for the mixing in past waste dissolution tests, or for percolation through pores in tests of that type, making it impossible to estimate the significance of mass-transfer limitation and scale up to other process conditions.

Recommendation: Dissolution tests should use a method that allows estimation of the mass-transfer effect, such as the rotating-disk method of Alkattan et al. (1997). These would be, by definition, simulant tests; the disk would be a pure fluoride salt solid and the solvent would be water, inhibited water, or waste liquid simulant. This particular form of apparatus, if feasible with fluoride salt solids, would simplify removing liquid samples at defined contact times, as liquid would not be part of a suspension requiring centrifugation.

Gap: The dissolution rate tests were not conducted on samples where other salts were largely absent, such as high-fluoride wastes or waste heels. These may be difficult to dissolve, since slow dissolution has been observed in a high-villiumite sample from AW-105, and in fine-grained residual solids in an AW-103 liquid sample after it was boiled down and re-diluted to its original concentration.

Recommendation: If these high-fluoride solids are of process significance, and actual waste tests are possible, new sample dissolution tests should include dissolution measurements made when only high-fluoride solids are present.

From Section 7:

Results: A model of mass-transfer rates for fluoride salt dissolution into water was developed and used for villiumite (NaF) and natrophosphate [$\text{Na}_7\text{F}(\text{PO}_4)_2 \cdot 19\text{H}_2\text{O}$]. In the latter case, a limitation of the model is that it is likely to be less applicable to double salts (three ions diffusing) than single salts. The solid/water ratio was set at the value that would give saturated concentration at 100% dissolution. Two slip-velocity assumptions were tested: unhindered terminal velocity (believed to be a lower bound for suspended particles) and zero velocity (molecular diffusion). At terminal velocity, the time to 99% dissolution was 2 to 5 min for 100- μm particles, 0.7 h for 2-mm particles, and 2 h for 6-mm particles. Under stagnant conditions, the time was 4 to 10 min for 100- μm particles, 1 day for 2-mm particles, and 9 days for 6-mm particles.

Gap: The model considers only one particle size, while actual fluoride salt waste contains polydisperse particles. Smaller particles would be expected to dissolve first, hindering the dissolution of larger ones.

Gap: The model has been applied with only one solid/liquid ratio (minimum water for dissolution) and only one initial salt concentration (zero).

Gap: The “diffusion coefficient for the solid” used in modeling represents a combination of the diffusion behavior of the two or three ions into which the solid dissolves. These depend strongly on ionic concentration and the fluxes of other ions in the solution. A value of $1 \times 10^{-9} \text{ m}^2/\text{s}$ was used, but the actual value could be a factor of 2 different in either direction. Under stagnant conditions, the mass-transfer rate is directly proportional to the diffusion coefficient; at high slip velocity, the rate is proportional to the two-thirds power of the diffusion coefficient. Dissolution tests should use a method that allows estimation of the mass-transfer effect, such as the rotating-disk method of Alkattan et al. (1997), to reduce this substantial uncertainty.

Gap: The common-ion effect of other salts has not been accounted-for in the model because it assumes only one salt is present. The presence of, for example, sodium nitrate in the solvent would affect the equilibrium concentration of dissolved villiaumite and could also affect the diffusion coefficients of the fluoride salt ions. The model is suitable only for water solvent or very dilute supernatants or solutions (such as inhibited water). Some thought needs to be given to whether inputs to this model could be adjusted to roughly account for the equilibrium effect of common ions.

Recommendation: The suspended-particle mass-transfer model should be exercised to approximate the effects of polydispersity, solid/liquid ratio, diffusion coefficient, and common-ion effect. This parametric study would clarify the relative importance of these parameters.

Gap/Recommendation: The slip velocity of the particles is at least as important a parameter as the diffusion coefficient, but the distribution of velocities in the dissolution process is unknown. The process for dissolving fluoride salt waste in the tanks could be modeled using a fluid-dynamics simulator to estimate a distribution of slip velocities of particles and evaluate the ability of the process. However, this effort would require better definition of the mixing and dissolution system than is presently available. The usefulness of the effort depends on whether the values of time to dissolution that were calculated above for relatively small slip velocities would be long enough to impede operations.

Gap/Recommendation: No model for mass-transfer was developed either for percolation through waste pores or for sluicing of a hardpan waste surface. Model-based estimates of those types of dissolution processes, if desired, will require new mass-transfer model development.

Observation: The possible effect of surface-reaction limitation on villiaumite dissolution rate was assessed based on literature for water dissolution of sodium chloride (Alkattan et al. 1997), since no literature was found for villiaumite (NaF). Trace metal species that strongly complexed with chloride ion in solution, such as Cd and Pb at 0.01 M concentrations, were found to inhibit the surface reaction for sodium chloride. The inhibition was sufficient that surface reaction, rather than mass-transfer, would be the controlling mechanism for 100- μm sodium chloride particles at terminal velocity. At slip velocities higher than terminal velocity, other trace metals tested by Alkattan et al. (1997) also had the potential to limit the sodium chloride dissolution reaction. If trace metals also inhibit villiaumite surface dissolution, increased agitation would not increase the dissolution rate in the tank.

Gap: The effect of trace constituents on fluoride salt dissolution is unknown.

Gap: No information was found to establish the effect on surface reaction of relatively high concentrations of typical waste anions such as nitrate, nitrite, and hydroxide, among others. The potential for these anions to affect surface-reaction dissolution rates – by, for example, occupying surface dissolution sites or complexing surface ions – is unknown.

Observation: For sodium chloride, and perhaps analogously for villiaumite (NaF), the surface-reaction dissolution rate in water was found to decrease linearly as the solution concentration went from 0% saturation toward 100% saturation. When a trace concentration of Cd was present in the solvent, the dissolution rate was lower than the linear dependence that existed for pure water solvent.

Gap: For the double salts natrophosphate [$\text{Na}_7\text{F}(\text{PO}_4)_2 \cdot 19\text{H}_2\text{O}$] and kogarkoite (Na_3FSO_4), there is no information about the way in which the surface reaction rate depends on the saturation fraction. The dissolution rate for other minerals can be strongly non-linear, and there are cases where dissolution slows or stops well before saturation is approached. It is also possible for double salts to dissolve non-stoichiometrically during part of the dissolution period while producing stoichiometric solutions at saturation. Natrophosphate has exhibited this behavior during crystallization from simulants (Reynolds

and Herting 2016), and might do the same during dissolution. This non-stoichiometric release of fluoride or of the other anions could complicate flowsheet calculations.

Recommendation: There is no *a priori* basis for predicting the surface reaction rate of the fluoride salts, but it may be the determining mechanism in dissolution processes. The potential for surface-reaction control of dissolution can only be assessed through simulant testing, which would need to be confirmed by testing of one or more actual waste samples. Test simulants should include the common anions. Some of the dissolution tests of all three of the fluoride salts need to include trace metals in the test solvents, which could be accomplished either by the dissolution tests with actual waste or by using an already-accepted HLW liquid simulant that contains trace metals, if there is such a simulant. The metals that (a) form the strongest complexes with fluoride, sulfate, and phosphate, and (b) are likeliest to appear in waste solutions should be present in the test simulants. Sufficient data should be collected during dissolution tests to allow non-stoichiometric dissolution to be observed, if present.

9.0 References

Alkattan M, EH Oelkers, J-L Dandurand, and J Schott. 1997. “Experimental studies of halite dissolution kinetics, 1: The effect of saturation state and the presence of trace metals.” *Chemical Geology* 137:201-219.

ASME NQA-1-2000, *Quality Assurance Requirements for Nuclear Facility Applications*. The American Society of Mechanical Engineers, New York, New York.

ASME NQA-1-2008, *Quality Assurance Requirements for Nuclear Facility Applications*. The American Society of Mechanical Engineers, New York, New York.

ASME NQA-1a-2009, *Addenda to ASME NQA-1-2008*. The American Society of Mechanical Engineers, New York, New York.

Bolling SD, TM Ely, JS Lachut, and ME LaMothe. 2017. *Solid Phase Characterization of Tank 241-AP-107*. RPP-RPT-60365, Washington River Protection Solutions LLC, Richland, Washington.

Bolling SD, JG Reynolds, TM Ely, JS Lachut, ME Lamothe, and GA Cooke. 2020. “Natrophosphate and kogarkoite precipitated from alkaline nuclear waste at Hanford.” *Journal of Radioanalytical and Nuclear Chemistry* 323:329-339.

Bong EY. 2013. *Solid-liquid mass transfer in agitated vessels with high solids concentration*. Ph.D. Thesis, School of Civil, Environmental and Chemical Engineering, RMIT University, Melbourne, Australia.

Boudreau BP, FJR Meysman, and JJ Middelburg. 2004. “Multicomponent ionic diffusion in porewaters: Coulombic effects revisited.” *Earth and Planetary Science Letters* 222:653-666.

Britton MD. 2019. *Solubility Data Review*. RPP-RPT-60326, Rev. 3, Washington River Protection Solutions LLC, Richland, Washington.

Callaway WS. 2003. *Tank 241-S-102 Core Sample Dissolution Testing Report*. RPP-15940, Rev. 0, Fluor Hanford, Richland, Washington.

Callaway WS and HJ Huber. 2010. *Results of Physiochemical Characterization and Caustic Dissolution Tests on Tank 241-C-108 Heel Solids*. LAB-RPT-10-00001, Rev. 0, Washington River Protection Solutions, Richland, Washington.

Callaway WS, SM Morley, and EA Vickery. 2020. *Boildown Test Final Report: Qualification of Evaporator Feed from Tank 241-AW-103*. RPP-RPT-62042, Rev. 0, Washington River Protection Solutions LLC, Richland, Washington. (not yet published, provided by the author)

Camenen B. 2007. “Simple and General Formula for the Settling Velocity of Particles.” *Journal of Hydraulic Engineering* 133(2):229-233.

CRC. 1975. *CRC Handbook of Chemistry and Physics*, 56th Ed., CRC Press, Boca Raton, Florida.

Crundwell FK. 2017. “Path from Reaction Control to Equilibrium Constraint for Dissolution Reactions.” *ACS Omega* 2:4845-4858.

- Dorozhkin SV. 2012. "Dissolution mechanism of calcium apatites in acids: A review of literature." *World Journal of Methodology* 2:1-17.
- Fishwick RP, JM Winterbottom, and EH Stitt. 2003. "Explaining mass transfer observations in multiphase stirred reactors: particle-liquid slip velocity measurements using PEPT." *Catalysis Today* 79-80:195-202.
- Herting DL. 1999. *Saltcake Dissolution FY 1999 Status Report*. HNF-5193, Rev. 0, Numatec Hanford Corporation, Richland, Washington.
- Herting DL. 2000. *Saltcake Dissolution FY 2000 Status Report*. HNF-7031, Rev. 0, Fluor Hanford, Richland, Washington.
- Herting DL. 2001. *Saltcake Dissolution FY 2001 Status Report*. HNF-8849, Rev. 0, Fluor Hanford, Richland, Washington.
- Herting DL. 2002. *Saltcake Dissolution FY 2002 Status Report*. HNF-12145, Rev. 0, Fluor Hanford, Richland, Washington.
- Herting DL and DB Bechtold. 2002. *Tank 241-S-112 Saltcake Dissolution Laboratory Test Report*. RPP-10984, Rev. 0, Fluor Hanford, Richland, Washington.
- Herting DL, GA Cooke, and RW Warrant. 2002. *Identification of Solid Phases in Saltcake from Hanford Site Waste Tanks*. HNF-11585, Rev. 0, Fluor Hanford, Richland, Washington.
- Herting DL, GA Cooke, JS Page, and JL Valerio. 2015. *Hanford Tank Waste Particle Atlas*. LAB-RPT-15-00005, Rev. 0, Washington River Protection Solutions, Richland, Washington.
- Herting DL and DW Edmonson. 1998. *Saltcake Dissolution FY 1998 Status Report*. HNF-3437, Rev. 0, Numatec Hanford Corp, Richland, Washington.
- Herting DL and JG Reynolds. 2016. "The composition of natrophosphate (sodium fluoride phosphate hydrate)." *Environmental Chemistry Letters* 14:401-405.
- Huber HJ. 2013. *Laboratory Report on Performance Evaluation of Key Constituents during Pre-Treatment of High-Level Waste Direct Feed*. RPP-RPT-53688, Rev. 0, Washington River Protection Solutions LLC, Richland, Washington.
- Poisson A and A Papaud. 1983. "Diffusion Coefficients of Major Ions in Seawater." *Marine Chemistry* 13:265-280.
- Reynolds JG. 2018. "Salt Solubilities in Aqueous Solutions of NaNO₃, NaNO₂, NaCl, and NaOH: A Hofmeister-like Series for Understanding Alkaline Nuclear Waste." *ACS Omega* 3:15149-15157.
- Reynolds JG, GA Cooke, DL Herting, and RW Warrant. 2013. "Salt mineralogy of Hanford high-level nuclear waste staged for treatment," *Ind. Eng. Chem. Res.*, **52**(29): 9741-9751, ACS Publications, Washington, D.C.
- Reynolds JG and JD Belsher. 2017. "A Review of Sodium Fluoride Solubility in Water." *Journal of Chemical & Engineering Data* 62:1743-1748.

Reynolds J and D Herting. 2016. "Crystallization of Sodium Phosphate Dodecahydrate and Recrystallization to Natrophosphate in Simulated Hanford Nuclear Waste." Waste Management Symposia 2016, March 6-10, 2016, Phoenix, Arizona.

Tilanus SN, LM Bergman, RO Lokken, AJ Schubick, EB West, RT Jasper, SL Orcutt, TM Holh, AN Praga, MN Wells, KW Burnett, CS Smalley, JK Bernards, SD Reaksecker, and TL Waldo. 2017. *River Protection Project System Plan*, ORP-11242 Rev. 8, Office of River Protection, Richland, Washington.

Toghiani RK, VA Phillips, and JS Lindner. 2005. "Solubility of Na-F-SO₄ in Water and in Sodium Hydroxide Solutions." *Journal of Chemical and Engineering Data* 50:1616-1619.

Uytioco EM. 2015. *Tank Farms Waste Transfer Compatibility Program*, HNF-SD-WM-OCD-015 Rev. 38, Washington River Protection Solutions LLC, Richland, Washington.

Wells BE, DE Kurath, LA Mahoney, Y Onishi, JL Huckaby, SK Cooley, CA Burns, EC Buck, JM Tingey, RC Daniel, and KK Anderson. 2011. *Hanford Waste Physical and Rheological Properties: Data and Gaps*. PNNL-20646; EMSP-RPT-006, Pacific Northwest National Laboratory, Richland, Washington.

Distribution List

All distributions of the current report will be made electronically.

Washington River Protection Solutions

Benson, PA
Britton, MD
Cree, LH
Reynolds, JG
Vitali, JR
Wagnon, TJ
WRPS Documents (TOCVND@rl.gov)

Pacific Northwest National Laboratory

Arm, ST
Bottenus, CLH
Brouns, TM
Burns, CA
Daniel, RC
Fountain, MS
Mahoney, LA
Peeler, DK
Project File
Information Release

Pacific Northwest National Laboratory

902 Battelle Boulevard
P.O. Box 999
Richland, WA 99354
1-888-375-PNNL (7665)

www.pnnl.gov